NASA CR-72144

FINAL REPORT

GPO PRICE $ _____

CFSTI PRICE(S) $ _____

Hard copy (HC) 3.00

Microfiche (MF) 1.30

ff 653 July 65

RESEARCH & DEVELOPMENT IN CdS PHOTOVOLTAIC CELLS

BY

J. C. Schaefer, E. R. Hill, T. A. Griffin

Prepared For

NATIONAL AERONAUTICS AND SPACE ADMINISTRATION

June 28, 1965 to June 27, 1966

CONTRACT NAS-7631

THE HARSHAW CHEMICAL CO

N O T I C E

This report was prepared as an account of Government sponsored work. Neither the United States, nor the National Aeronautics and Space administration (NASA), nor any person acting on behalf of NASA:

A.) Makes any warranty or representation, expressed or implied, with respect to the accuracy, completeness, or usefulness of the information contained in this report, or that the use of any information, apparatus, method, or process disclosed in this report may not infringe privately owned rights; or

B.) Assumes any liabilities with respect to the use of, or for damages resulting from the use of any information, apparatus, method, or process disclosed in this report.

As used above, "person acting on behalf of NASA" includes any employee or contractor of NASA, or employee of such contractor, to the extent that such contractor prepares, disseminates, or provides access to, any information pursuant to his employment or contract with NASA, or his employment with such contractor.

Requests for copies of this report should be referred to:

National Aeronautics and Space Administration
Office of Scientific and Technical Information
Attention: AFSS-A
Washington, D.C. 20546

NASA CR-72144

FINAL REPORT
RESEARCH AND DEVELOPMENT
IN
CdS PHOTOVOLTAIC FILM CELLS

by
J. C. Schaefer, E. R. Hill, T. A. Griffin

Prepared For

NATIONAL AERONAUTICS AND SPACE ADMINISTRATION
June 28, 1965 to June 27, 1966

Contract NAS 3-7631

Technical Management
NASA Lewis Research Center
Cleveland, Ohio
Space Power Systems Division
Clifford Swartz

Harshaw Chemical Company
Crystal-Solid State Division
1945 E. 97th Street
Cleveland 6, Ohio

FOREWORD

This report was prepared by the Crystal-Solid State Division of The Harshaw Chemical Company. The work has been sponsored by the Space Power Systems Procurement Section of the NASA Lewis Research Center with I A. E. Potter acting as Technical Advisor and Mr. Clifford Swartz acting as Project Manager.

Project direction has been provided by Mr. J. C. Schaefer with Mr. E. R. Hill and Mr. T. A. Griffin acting as principal investigators for the research and development work respectively. The following Harshaw personnel have contributed to this program: B. Keramidas, R. J. Humrick, R. W. Olmsted, D. J. Krus, W. Baldauf, N. E. Heyerdahl, P. J. Marn, and C. A. Morano. Dr. N. K. Pope of the Royal Military College of Canada served as consultant.

List of Tables

List of Figures

Table of Contents

Abstract

Additional research and developmental studies were made on the CdS thin film solar cell. Several previously unreported cell characteristics are discussed, such as I-V curve hysteresis, reversible changes due to forward and reverse bias, changes of spectral response with temperature and bulk properties, and cell capacitance as a function of reverse bias. These results lend support to the E. Hill [1] CdS solar cell model. Vapor transported CdS film, high reliability electroplated grid collectors and CdS surface treatments are also discussed. Highest reported cell energy conversion efficiency for the contract period was 6.9%.

Summary

A large advance has been made toward determination of cell characteristics and understanding of the mechanism of the CdS thin film solar cell. Progress was implemented with the development of the basic CdS solar cell model. (1)

Cell current voltage curves show hysteresis is cell dependent and will vary according to the cell fabrication methods used. This investigation led to the discovery that an operating cell can be physically changed by applying a forward current density of 10ma/cm^2 in the dark. A greatly reduced output results. Reverse current will cause a return to the original values. Increase in temperatures from 200°K to 400°K shows a decrease in quantum yield. Weighing of the total amount of barrier layer material formed has established that the barrier is a cuprous sulfide and that copper has a diffusion constant of 8×10^{-10} cm^2/seconds at 70°C.

Data obtained from capacitance measurements of CdS with 10^{15} to 10^{17} electrons/cm^3 carrier concentrations imply a cell model of p-type Cu_2S overlaying n-type CdS with the depletion region almost totally in the CdS.

The development areas show that silver serves well as an interface material between the substrate and the CdS, but is not essential. Surface treatment of the CdS film before barrier formation by etching is essential for higher cell

efficiencies. Various fabrication improvements are discussed. Improvements have been made in electrodeposition of the collector grid. Previous reports gave a maximum efficiency of about 3.5%, while the maximum for this period was 4.7%. A thermal-compression method for applying an electroformed grid is reported.

The closed-space vapor transport procedure for formation of CdS thin films has overcome a major adherence problem and is capable of reproducing films of a given quality.

The pilot line reports a maximum cell conversion efficiency of 6.9%.

Test cells gridded by electrodeposition and thermo-compression have withstood NASA environmental thermal cycling equivalent to over one (1) year in space without degradation.

Introduction

Interest in the thin film cadmium sulfide solar cell continues because the cells have greatly improved in reliability and have shown improvement in cell efficiency.

Previous work on this contract has resulted in the publication of the E. Hill [1] model for the CdS solar cell. This basic model describes mechanisms and characteristics previously unrecognized. Studies made during the contract year show that the barrier is p-type cuprous sulfide on n-type cadmium sulfide and that the junction is in the p-type material. Ion migration is a factor in cell manufacture and the diffusion constant of copper at 70°C has been measured. Carrier concentration in the CdS has an effect on the spectral response.

Establishment of the proper conditions through research are expected to provide the ultimate answers to methods of fabrication for attainment of maximum cell efficiency and cell life.

Two methods of applying reliable collector grids to the barrier surface are reported. The electrodeposition method has been improved through better resist techniques and use of a gold alloy. Thermo-compression bonding of electroformed grids by high pressures of about 3000 p.s.i. at laminating temperatures appears to be competitive. The latter method is rapid and requires no adhesives. Both methods eliminate encapsulation as a means for grid attachment.

Vapor transport has been shown to be a simple process in which film properties can be controlled.

I-V Curve Measurements and Hysteresis

Clues to the mechanisms involved in the CdS solar cell can be obtained by a study of the current-voltage data. Generally the device can be described by the diode equation:

$$I = I_o \left[(\exp \frac{qV}{KT}) - 1 \right]$$

with appropriate allowances for series and shunt resistance effects. The term, I_o, is the leakage current, is temperature dependent, and is determined by the materials on each side of the junction. To explain deviations in the negative voltage region, it is sometimes assumed that I_o is also voltage dependent. In any case, it is clear that this is an equation of state for the device and uniquely determines I at any particular voltage and temperature. The q is the electronic charge, V is the voltage, K is a constant, while T is the temperature in ^oK. However, referring to Figure 1, it can be seen that the I-V curve for a typical CdS cell is not single valued when traced at the rate of 1 cycle in 48 hours. It is important to determine whether this hysteresis exists in the steady state or is simply a long term transient phenomenon. I-V curves have been measured at various frequencies and analysed. An x-y plotter was used to record the data. A DC power supply fed from a motor driven variac served as the low frequency ramp function generator. All data were taken in the dark at room temperature. The results show that at frequencies above 10 sec^{-1}, the cell behaves as a normal diode and can be described as a rectifier with a parallel capacitance of 10^{-1} to 10^{-2} microfarads per cm^2. As frequency is decreased, another effect sets in, with the behavior shown in Figure 1. This hysteresis effect increases at the frequency

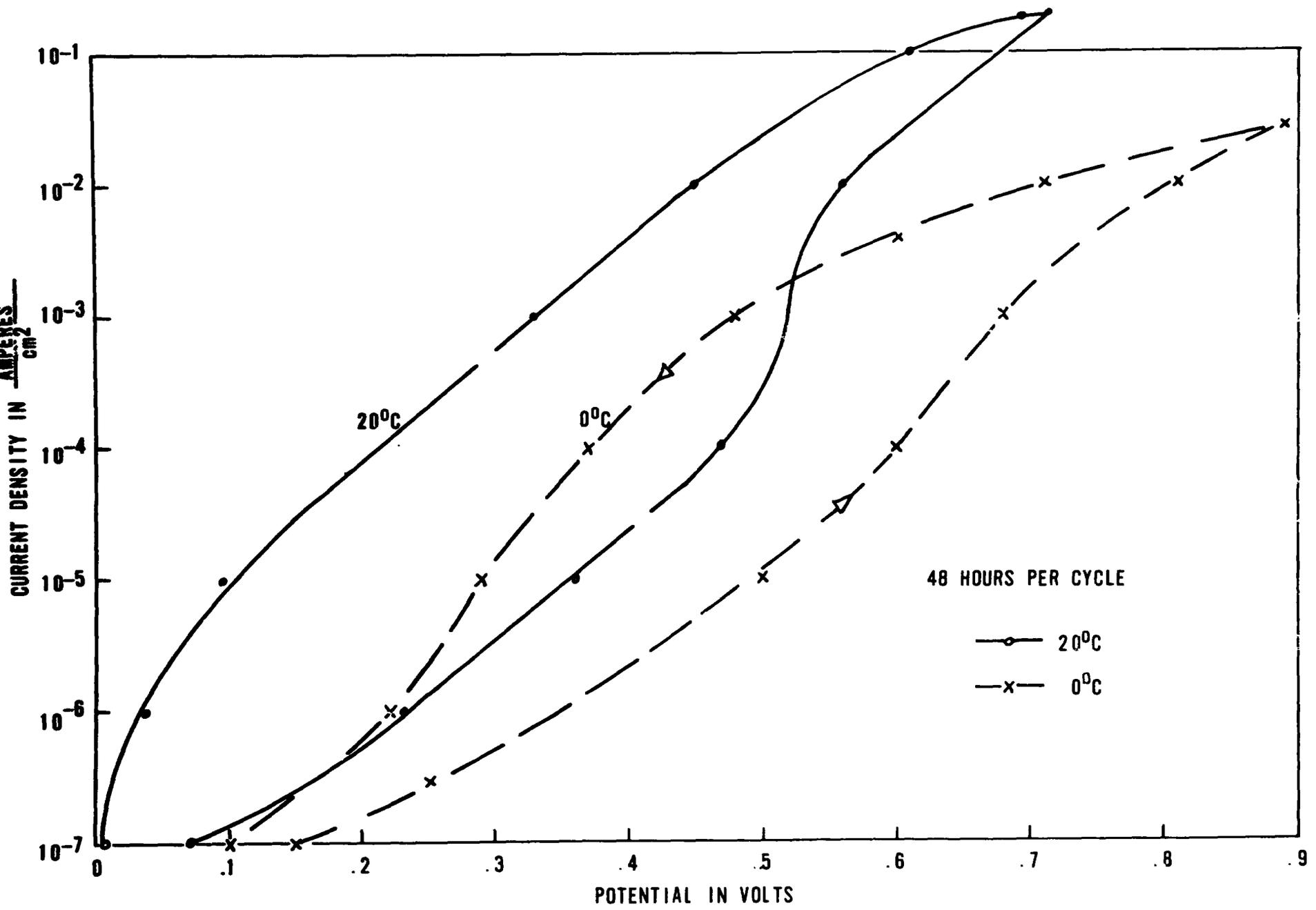

Figure 1 DARK I-V CURVES FOR CELL X39.31-2

decreases and is a function of the maximum voltage applied to the cell. The effect seems to be only weakly temperature dependent as shown in Figure 2. It also seems to be greatly dependent on cell processing, as different heating cycles change the observed behavior. The hysteresis curve obtained from a given cell can be changed by varying the heat treatment. The investigation has not progressed to the point at which the curves can be used to predict cell behavior. More data is being gathered on the low frequency dependence over the range from 10^{-2} sec^{-1} to 10^{-6} sec^{-1}. Whatever the microscopic nature of the mechanism for the effect, two facts are clear: 1) If the hysteresis is in fact a steady state phenomenon, as in the case of ferromagnetism, a change of state must occur in the material of the cell. This change must be characterized by an energy which can be measured by the I-V data itself; 2) If the hysteresis is a transient effect, such as shown by RC and LC networks, a low frequency limit exists and it too should be shown in -the I-V data. Indications are that the latter case is true, and that it is a slow transient effect due to the motion of the ions.

Charge Separating Mechanism and Cell Reversibility

To examine the charge separating mechanism, or the junction, data on I-V curves has been taken. As noted in the preceeding section, an effect of hysteresis was evident in the I-V curve. When the curve was traced at a finite rate, the ascending and

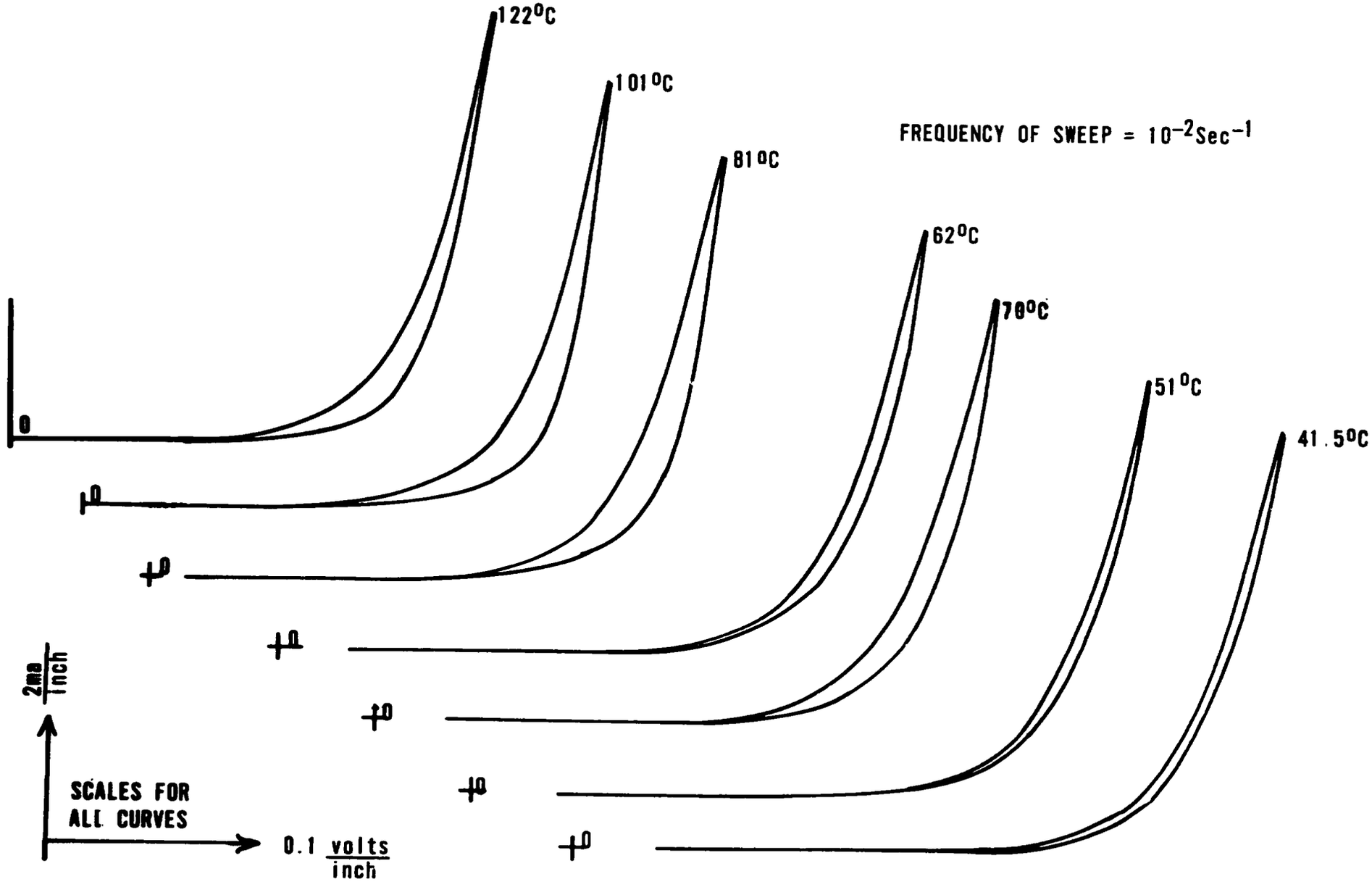

FIGURE 2 DARK I-V CURVES FOR CdS SOLAR CELL

decending branches were separated. It was also noted that a normal cell could be physically changed by applying a forward or reverse bias in the dark with a 60 cycle sweep voltage.

For the experiments, a cell was connected to a constant current source and a 10 ma/cm^2 forward current was passed through for 24 hours. Figure 3-b shows the I-V curve after the 24 hours. The current was then reversed. The voltage across the cell rapidly increased, was adjusted to 5 volts and reapplied for 24 hours. Figure 3-c shows the I-V curve after this biasing. The process appears to be reversible. During this test, another effect was noted. If the forward bias of a cell was removed after an extended time period and the cell was short circuited, a current would flow. In fact, power could be extracted from the cell. To study this further, the cell was biased in the forward direction and allowed to come to a steady state. It was then shorted and the current drawn was recorded as a function of time. The time dependence appeared to be the sum of two decreasing exponentials.

Table I shows the pertinent data for two cells so tested. Note the long time constants involved which indicate that relatively immobile charge carriers are involved. If this effect is the result of motion of ions in the space charge region, a few calculations are in order.

Assuming that the ions are singly charged, then the forward bias causes a drift and a separation of the ions into a dipole layer. The negative ions are large compared to positive metal ions and, therefore, are considered essentially

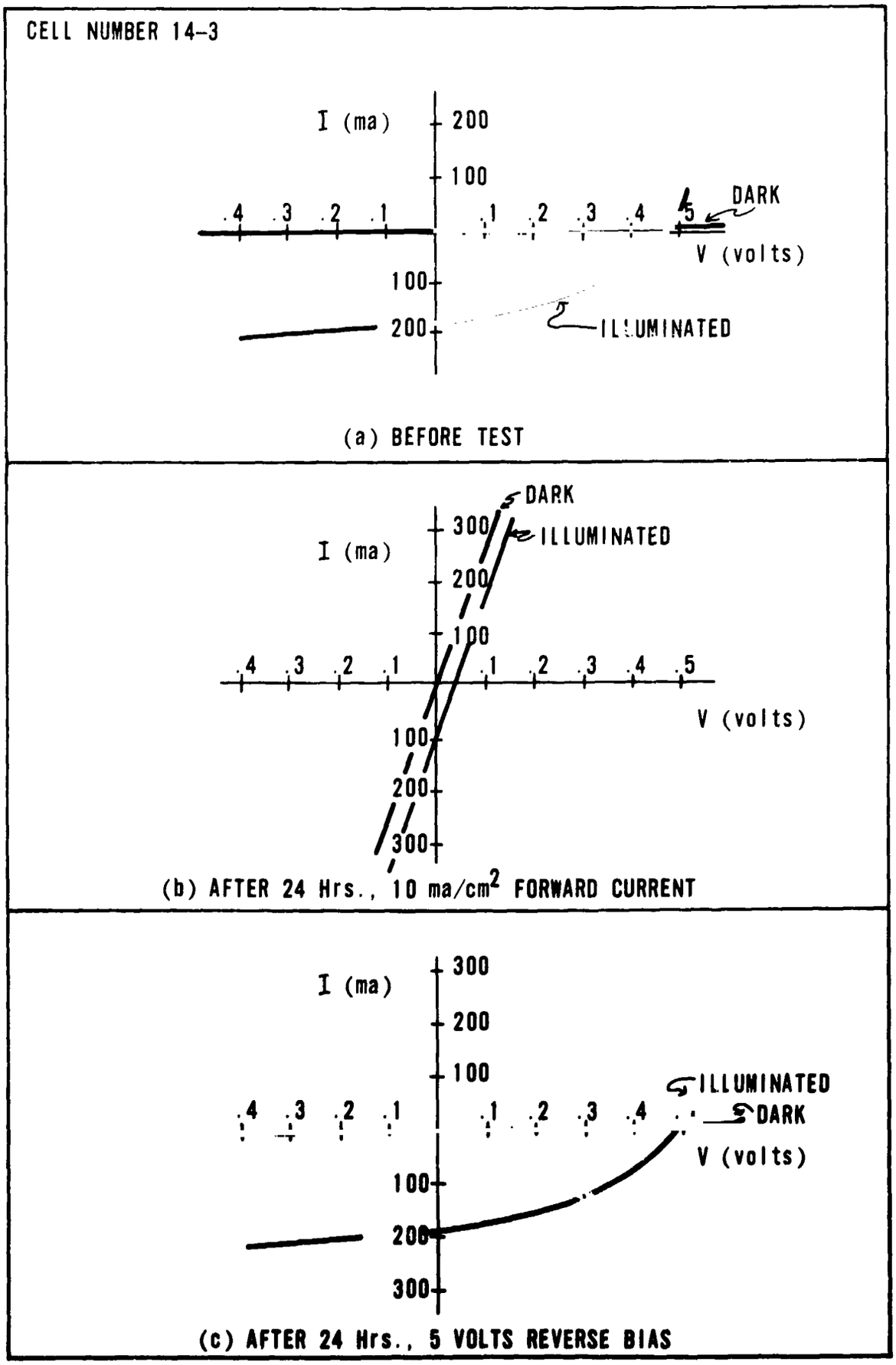

Fig. 3 REVERSIBLE CHANGES DUE TO APPLIED BIAS

TABLE I - Bias Effects Data

	Forward Bias Voltage Time-Hours	I^{**}_{sc} Amperes	T 1 Minutes	T 2 Minutes	Steady State Bias Voltage Volts	Steady State Bias Current Milliamperes	Extracted Charge μCoul.	Open Circuit Voltage* Millivolts
Cell # 1	0.5	7×10^{-8}	2.8	9.2	.455	2.0	29	49
	72	6×10^{-8}	6.1	7.3	.45	2.7	29	13
	7	1.23×10^{-7}	2.1	6.4	.44	2.4	28.5	35
	16	1.41×10^{-7}	2.3	12.0	.49	10.0	91	30
	5	3.3×10^{-7}	2.1	10.8	.495	9.8	120	44
	0.5	5.3×10^{-7}	1.0	5.0	.52	9.0	78	95
	3	8.2×10^{-8}	2.9	10.4	.475	10.0	36	0.2
Cell 1A	16	1.3×10^{-7}	3.0	22.0	.46	11.1	105	0.4
	2	2.0×10^{-7}	1.6	10.6	.505	8.3	83	1.0

Electroformed Grid Cells

* Voltage appearing across cell immediately after removing bias

** Current generated by cell immediately after removing bias

fixed. When the cell is shorted, it behaves as a condenser with a stored charge. The current flowing can be related to the charge remaining by

$$I = \frac{Q}{\tau} = \text{Current}$$

Q = Charge

τ = Discharge time constant

Assume also that the charge Q is accumulated in two sheets (positive and negative) separated by a distance W in a material where the ion diffusion constant is D

Then,

$$\tau = \frac{W^2}{D}$$

W = spacing of charge sheets

D = diffusion constant

By the Einstein relation

$$D = \frac{\mu kT}{q}$$

μ = ion mobility

k = Boltzmann's constant

T = absolute temperature

q = electronic charge

So that

$$\tau = W^2 q/\mu$$

$$\mu = W^2 q/\tau kT$$

Using the second set of data points with approximately equal time constants for the two ions, and assuming the charge separation is 10^{-4}cm

$$\tau_1 = 6.1 \text{ minute}$$

$$\tau_2 = 7.3 \text{ minute}$$

$$W = 10^{-4}\text{cm}$$

we find

$$\mu_1 = 10^{-9}\text{cm}^2/\text{volt second}$$

$$\mu_2 = 9 \times 10^{-10}\text{cm}^2/\text{volt second}$$

The effect of power extraction after application of forward bias is also recognized as persistent internal polarization, which was seen in CdS some time ago. (2) The diffusion constants are:

$$D_1 \quad (20°C) = 2.7 \times 10^{-11}\text{cm}^2/\text{sec.}$$

$$D_2 \quad (20°C) = 2.3 \times 10^{-11}\text{cm}^2/\text{sec.}$$

Diffusion constant data on cadmium and copper in CdS or Cu_2S is sparse but these numbers are among those reported. (3) This is the same order as lithium in silicon, and implies that the junction will be affected by the motion of ions in the field regions.

Light Absorbing Material in the Junction Region

Absorption was examined in respect to the temperature dependence of the spectral response of the cell. A chemiplated 3.5% efficient cell laminated in Mylar was mounted on a small hot plate which was placed at the exit slit of a monochromator. Spectral response was then measured at 200°K, 300°K, and 400°K. The data are shown in Figure 4. The significant features are as follows:

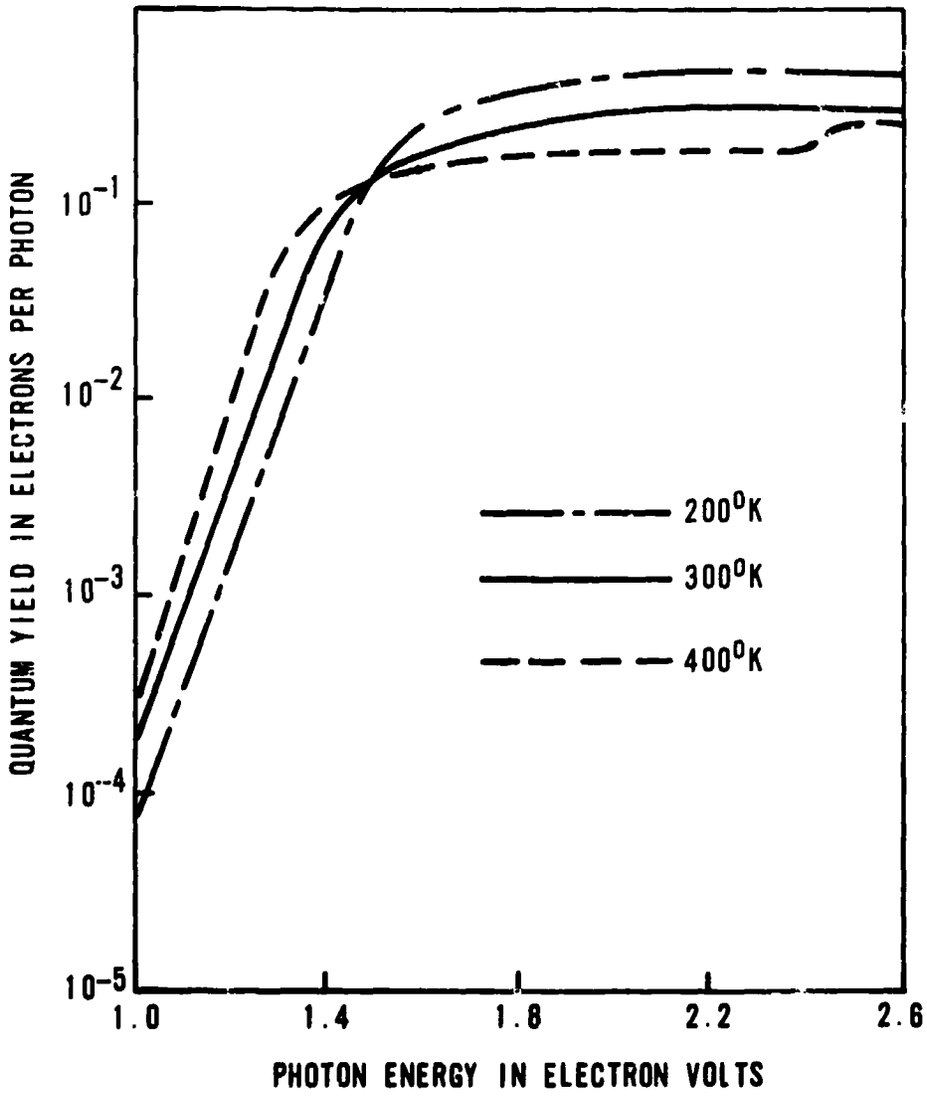

Fig. 4 TEMPERATURE VARIATION OF CdS SOLAR CELL SPECTRAL RESPONSE

1. At the low energy limit, the change in response is that due to the temperature dependence of the bandgap. That is, the temperature increases, while the bandgap decreases at the rate of about 10^{-3} eV per °K. The slope should also change as the reciprocal of the absolute temperature, but the noise level obscures this small effect.
2. For energies between about 1.4 and 2.4 eV the quantum yield decreases with increasing temperature.
3. At temperatures around 400°K, a step is seen at 2.4 eV which is not present at lower temperatures.

The effects in 2 and 3 can be explained by examination of the chemical reaction which is used to make the cell, which is:

$$Cu_2Cl_2 + CdS \rightleftarrows Cu_2S + CdCl_2$$

$$\Delta F^\circ \ (298°K) = -12 \ \frac{k \ cal}{Mole}$$

$$Ln \ \frac{[Cu_2S]}{[Cu_2{}^{+2}]} \ \frac{[Cd^{+2}]}{[CdS]} = \frac{-\Delta F^\circ}{RT}$$

If Cu_2S is assumed to be the active material for photons in the range from 1 to 2.4 eV, then the quantum yield will be temperature dependent. As the temperature increases, the right-hand term becomes a smaller number, and the concentration of Cu_2S decreases. Likewise, the CdS concentration in the region of the cell surface increases with increasing temperature, resulting in the step at 2.4 eV at higher temperatures.

The net result of increasing temperature is to cause a decrease in sunlight generated current. The loss in response

between 1.4 and 2.4 eV far outweighs the gain due to the decreased bandgap. The change appears to be linear over this temperature range. The open circuit voltage also decreases linearly with temperature, at the rate of above 1 millivolt per °K. These two effects are shown in Figure 5. If the fill factor remains constant, power will vary parabolically with temperature. For small changes in this range the quadratic term is small and a linear function is a close approximation with a coefficient of the sum of the rates of change of voltage and current. This can be expressed analytically as follows:

$$I = I_o - \frac{dI}{dT} T = \text{short circuit current}$$

$$V_x = V_o - \frac{dV}{dT} T = \text{open circuit voltage}$$

$$\text{Power} = IV = I_o V_o - V_o \frac{dI}{dT} - I_o \frac{dV}{dT} T + \frac{dI}{dT} \frac{dV}{dT} T^2$$

The last term is small so,

$$P = IV \simeq I_o V_o - V \frac{dI}{dT} - I_o \frac{dV}{dT} T$$

$$\frac{dP}{dT} = V_o \frac{dI}{dT} - I_o \frac{dV}{dT}$$

$$\frac{1}{I_o V_o} \frac{dP}{dT} = -\frac{1}{I_o} \frac{dI}{dT} - \frac{1}{V_o} \frac{dV}{dT}$$

Thus, the fraction change in power is the sum of the fractional changes in current and voltage. Using the data shown in Figure 5, this results in a fraction rate of change of power at room temperature of

$$\frac{1}{P} \frac{dP}{dT} = 4 \times 10^{-3} \text{ / °K at 300°K}$$

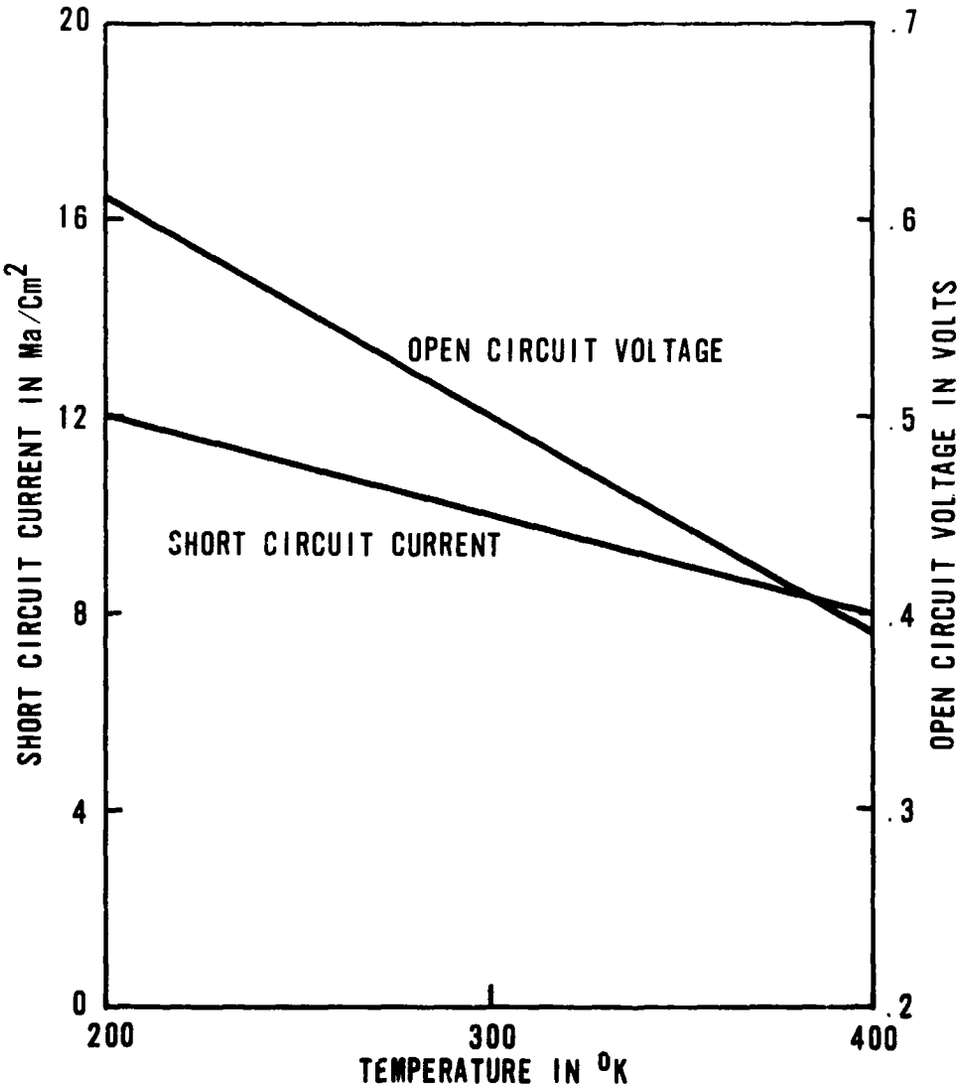

Fig. 5 TEMPERATURE DEPENDENCE OF OPEN CIRCUIT VOLTAGE AND SHORT CIRCUIT CURRENT FOR CdS SOLAR CELL

Cu_2S Formation and Diffusion

To further the study of the nature of the junction in the CdS cell it is necessary to determine the nature of the Cu_2S layer. This layer is formed chemically when the CdS film is immersed in an aqueous CuCl solution. By the nature of this process one expects two major features to be apparent. First, the chemical reaction in the solution is governed only by the concentration of the active agent in the liquid and the surface concentration of the reaction product on the CdS film. Secondly, the distribution of Cu_2S in the bulk CdS is governed by physical diffusion as a result of concentration gradients. This can all be stated analytically in the following equations. First, the chemical reaction is

$$Cu_2Cl_2 + CdS \rightleftarrows Cu_2S + CdCl_2$$

Next, since the reaction concerns two components, its rate is proportional to the product of their concentration

$$\frac{d}{dt}\,[Cu_2S \text{ concentration}] = \alpha\,[Cu_2Cl_2 \text{ concentration}]\;\;[CdS \text{ concentration}]$$

where α = proportionality constant which may be temperature dependent

Finally, in the bulk, the diffusion equation holds, and treating this as one dimensional problem,

$$D\,\frac{\partial^2 C}{\partial x^2} = \frac{\partial C}{\partial t}$$

C = concentration of the diffusing specie,

D = diffusion constant of specie, which is temperature dependent, and

X = diffusion depth

If the following notation is adopted;

where C = concentration of Cu_2S,

C_o = bulk concentration of CdS, and

C_L = concentration of Cu_2Cl_2 in liquid is taken to be a constant,

then,

$$\frac{d}{dt} C(x = 0,t) = \alpha C_L \quad [C_o - C(x = 0,t)]$$

$$C(0,t) = C_o \quad [1 - e^{-C_o C_L t}]$$

The diffusion equation is then solved using this as a boundary condition for x = 0; and C(x,0) = 0 for all x.

The solution for the boundary conditions is rather involved, and the details are shown in the appendix. This solution gives an expression for (C(x,t). In the present device, determination of the profile of the Cu_2S in the CdS film is difficult, and an easier technique is to determine the total amount of Cu_2S incorporated in the film. This is represented as

$$M(t) = \int_o^\infty C(x,t)dx$$

The technique for measurement of this quantity is as follows. A CdS film of known area is weighed. It is then chemiplated for a known length of time to form the Cu_2S layer. It is then etched in a water solution of KCN to remove the Cu_2S and the water soluble reaction products. It is then dried and weighed again. The difference between the two weights represents the amount of CdS which entered into the reaction and produced Cu_2S. Thus, it is proportional to the mass of Cu_2S formed. The analytic expression for the integral is formidable, and so we look only at the asymptotic expressions for long and short immersion times. In these cases, the integrals can be evaluated easily. The results are:

$$M(t) = At^{3/2} \text{ for short times}$$

where

$$A = \frac{8C_o D^{5/2}}{\lambda \sqrt{\pi}}$$

and

$$M(t) = \frac{2C_o D^{1/2}\ t^{1/2}}{\sqrt{\pi}} \text{ for long times}$$

Figure 6 shows the time dependence of total mass for three temperatures. At short times, the $t^{3/2}$ dependence holds, and since the solution is saturated, the λ term will be temperature dependent along with D. These will both cause the reaction rate to increase with temperature at shorter times. At longer times, the total mass should depend only on the diffusion constant. To reach these, however, a rather thick Cu_2S layer is required and the differences in density between Cu_2S and CdS results in high stresses and spalling of the Cu_2S layer,

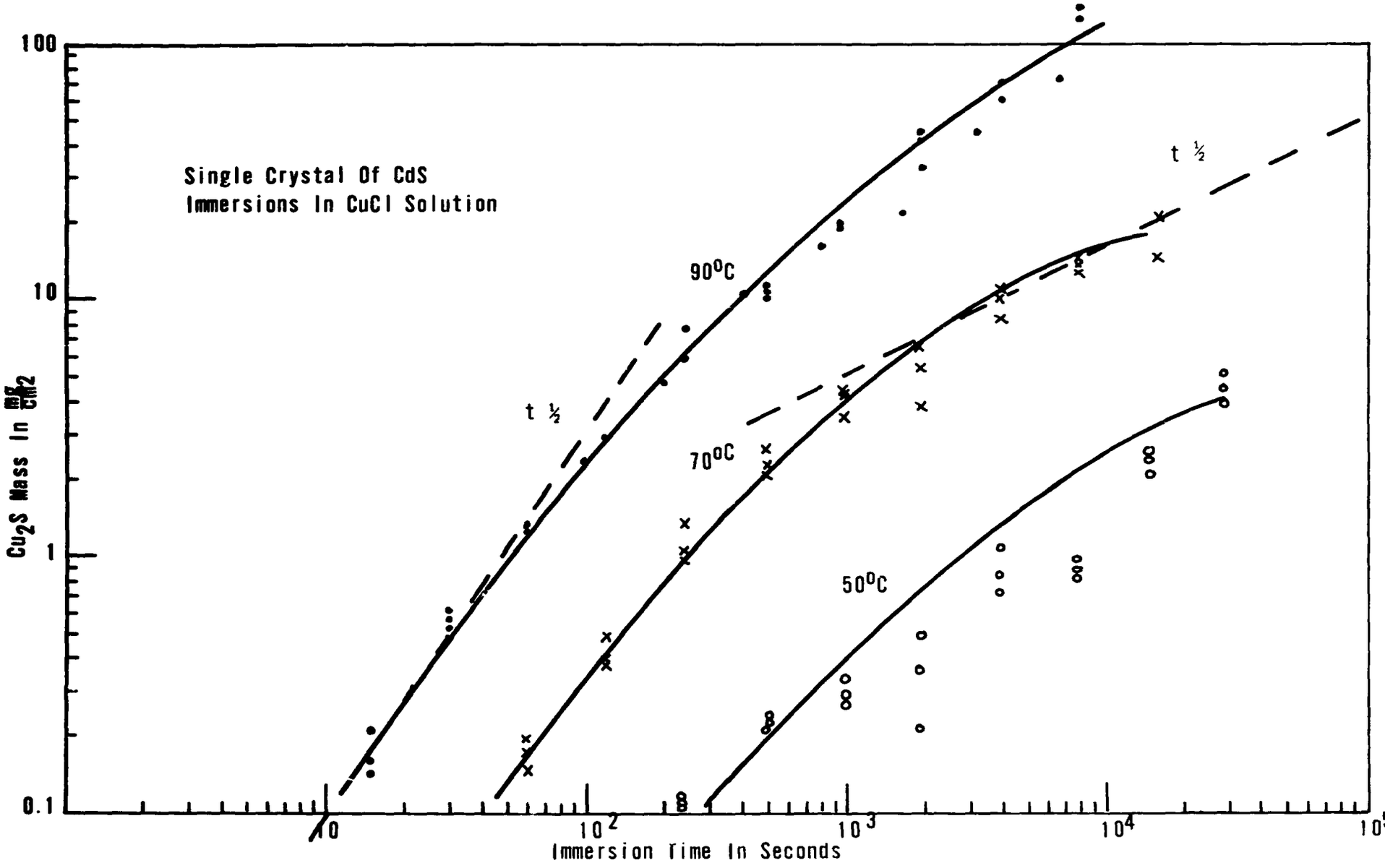

Figure 6 Cu_2S Layer Formation In CdS

thus, the long time data here is not too reliable at 90°C. Using the 70°C data at long time we find:

$$D(70°C) = 8 \times 10^{-10} \text{ cm}^2/\text{sec.}$$

This is rather high compared to the value measured by the reversible ion diffusion but is within reasonable agreement considering the differences in the methods.

Finally, from this experiment, it is established that Cu_2S is the reaction product. According to the equation,

$$Cu_2Cl_2 + CdS \rightleftarrows Cu_2S + CdCl_2$$

one atom of Cd is replaced by two atoms of Cu. Thus, for each mole of Cu_2S formed, the film will gain 14.68 grams in mass. If the mole of Cu_2S is etched off, the film, will lose 159.15 grams mass. Adopting the following nomenclature,

m (bare) = initial CdS film mass

m (plated) = mass of film after chemi-plating reactions

m (etch) = mass of film after KCN etch

M = number of moles of CdS in the reaction

Then

m (plated) - m(bare) = M(14.68) gm

m (bare) - m(etch) = M(112.4) gm

$$\frac{\text{m (bare) -m (etch)}}{\text{m (plated) -m (bare)}} = 7.67$$

If the quantities in the numerator and denominator are measured and plotted, the results appear as in Figure 7.

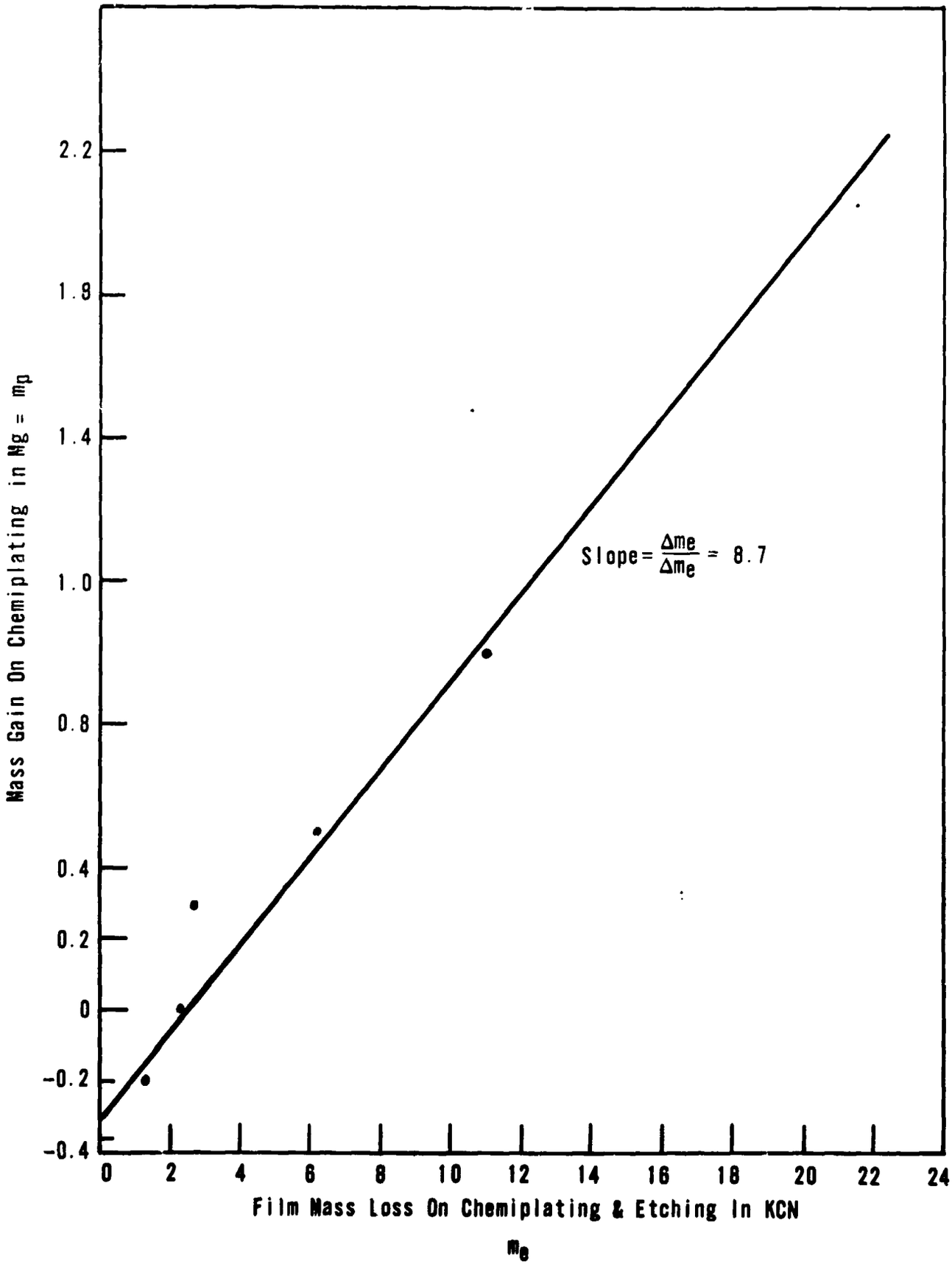

Figure 7 Mass Change For CdS Chemiplated Films

The dependence, first, is linear, and secondly indicates a slight error in the zero of the balance. The measured slope is 8.7 and indicates that not quite two coppers replaced each cadmium. In fact, the ratio is,

$$\frac{2(7.67)}{8.7} = 1.77$$

almost exactly the correct ratio for digenite or $Cu_{1.8}S$. It clearly shows that the product is not CuS.

Spectral Response and Junction Characterization

An investigation of the dependence of cell properties on the bulk CdS carrier concentration was made. For this work single crystal slabs of CdS with known electron concentrations were chemiplated with predetermined amounts of Cu_2S. The CdS was contacted with indium mercury amalgam and the Cu_2S with a taped-on gold grid. The cells were not heated. The spectral responses were measured and the results appear in Figures 8,9, and 10. Figure 8 shows the responses for a set of crystals with 10^{15} electrons/cm^3. The Cu_2S thicknesses range from 5×10^{-6}cm to 3×10^{-4}cm.

Capacitance measurements were also made and Figure 11 shows the data for the crystal with 5×10^{-6}cm of Cu_2S on CdS with 10^{15} carriers/cm^3 (by Hall measurement). $\frac{1}{C}$ was plotted as a function of reverse bias potential. The linear dependence indicates an abrupt junction. The calculated carrier concentration from the slope is $1.3 \times 10^{16}/cm^3$.

The Hall measurement for carrier concentration was made on a sample from the same CdS ingot, but not the particular piece used for the cell. This may explain the discrepancy between the Hall data and capacitance data for carrier concentration. Measurements on the other cells of Figure 8 also show abrupt junctions with carrier concentration in the same region.

These data imply a model of p-type Cu_2S overlaying n-type CdS with the depletion region almost totally in the CdS, as shown in Figure 12. Photons with energy less than 2.3 eV are absorbed only in Cu_2S. The hole-electron pairs are collected only if they are generated in the depletion region. Consequently only a small fraction of the light absorbed in Cu_2S produces electrical current, and in fact, the Cu_2S acts mostly as a light absorber. At energies above 2.4 eV, photons produce hole-electron pairs in CdS also, and a sharp increase in response is seen. The maximum in response is limited by the thickness of the Cu_2S layer.

At energies greater than 2.4 eV, the response decreases due to the increasing absorption coeffecient of the Cu_2S. In this region, the absorption coefficient increases as $(E-Eg)^{1/2}$ due to the parabolic distribution of the density of states near the band edge. If the absorption coefficient of Cu_2S is known, the slopes of the response curves will allow calculation of the Cu_2S thickness. Absorption coefficient measurements on Cu_2S were not completed in sufficient time to correlate the data.

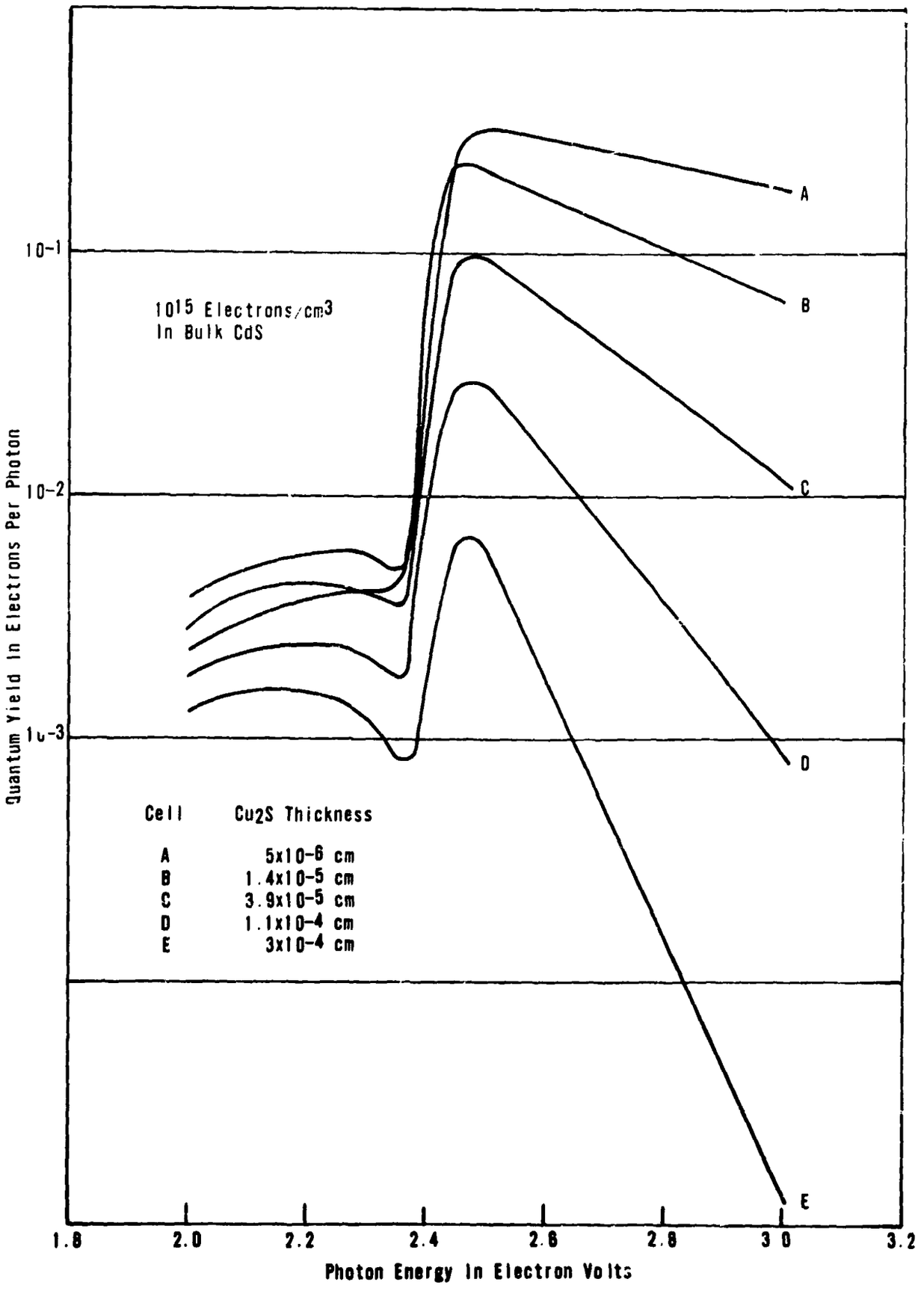

Figure 8 Monochromatic Spectral Response For 10^{15} Electrons Per cm^3 In Bulk CdS

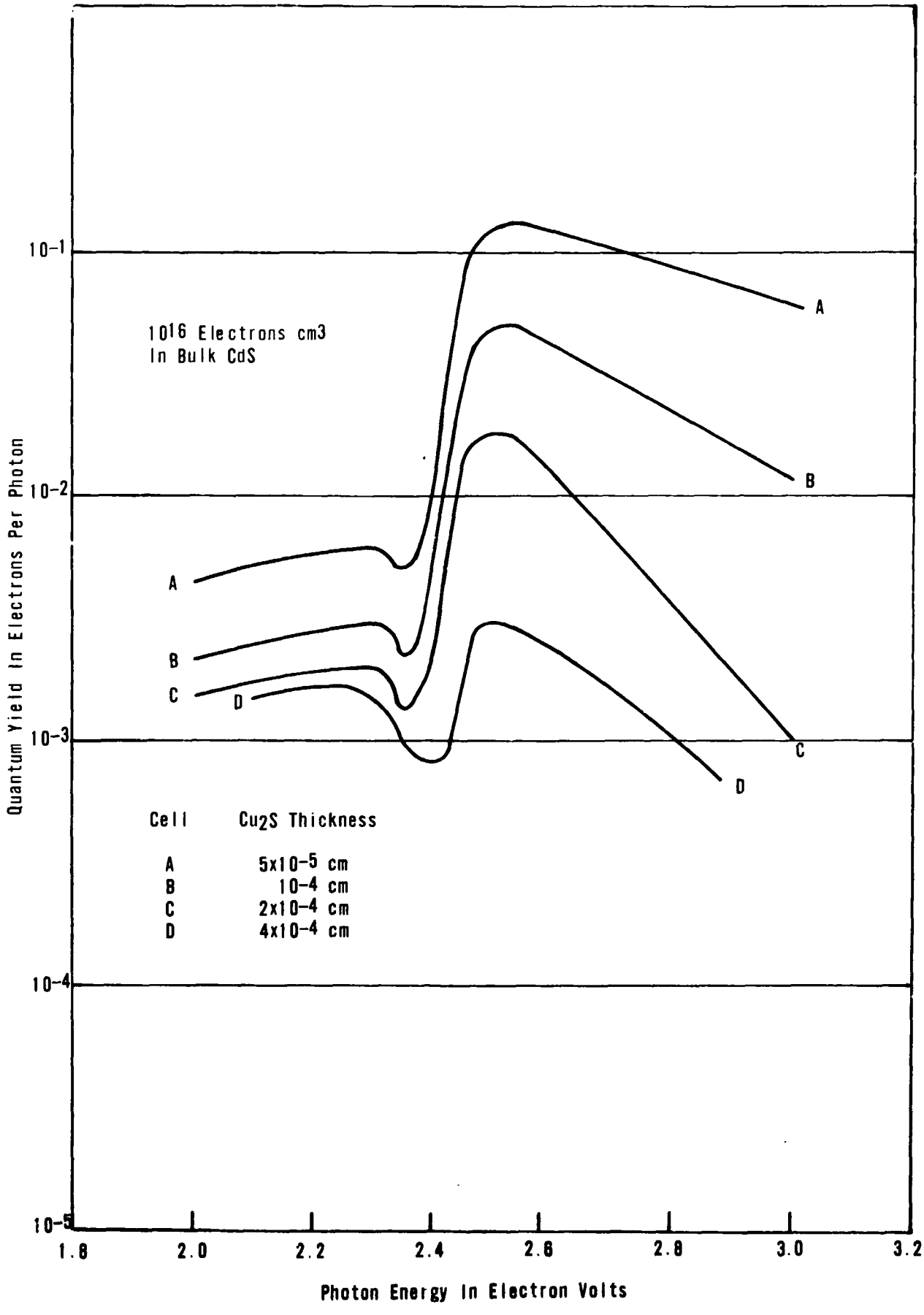

Figure 9 Monochromatic Spectral Response For 10^{16} Electrons Per cm^3 In Bulk CdS

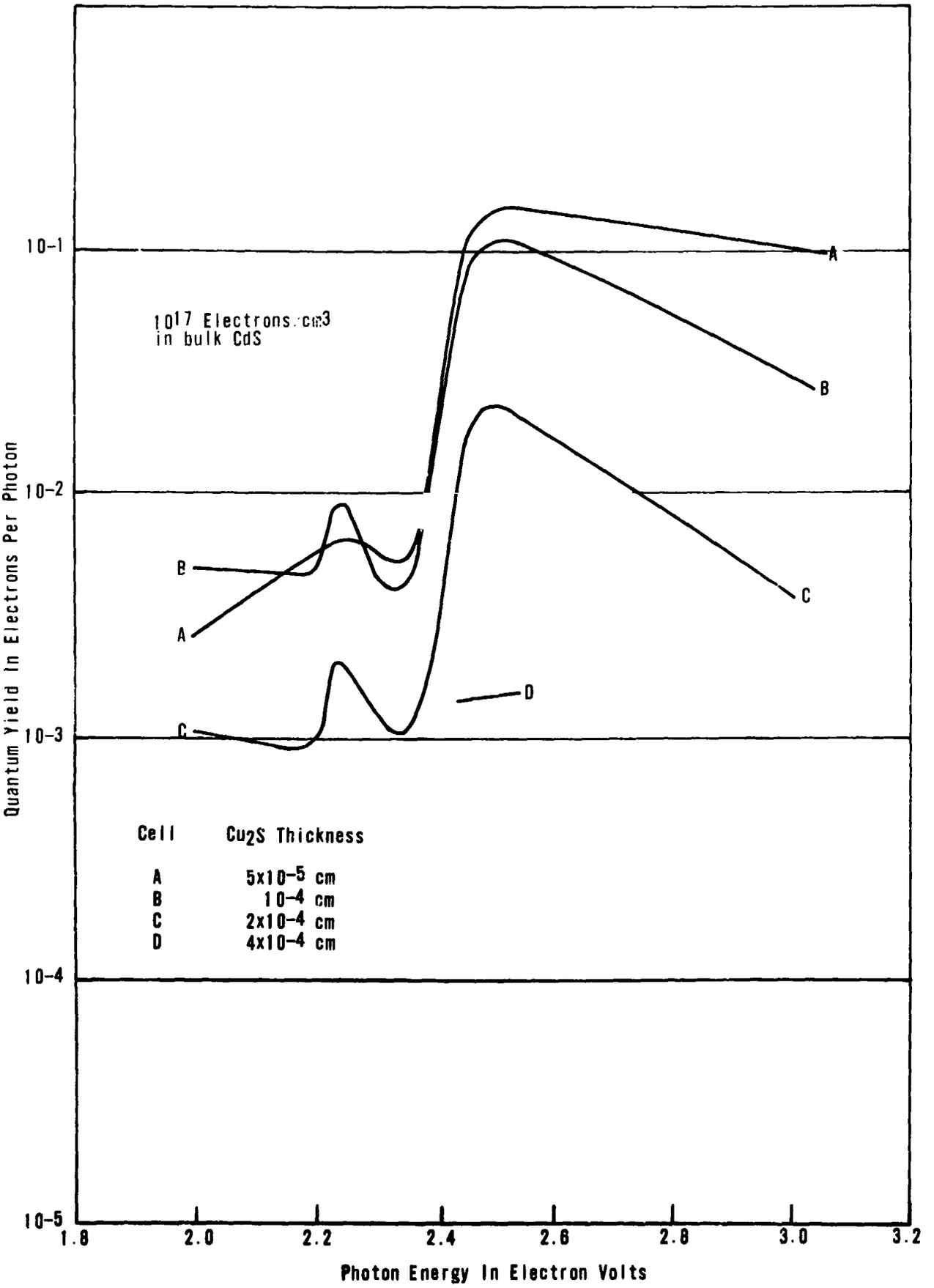

Figure 10 Monochromatic Spectral Response For 10^{17} Electrons Per cm3 In Bulk CdS

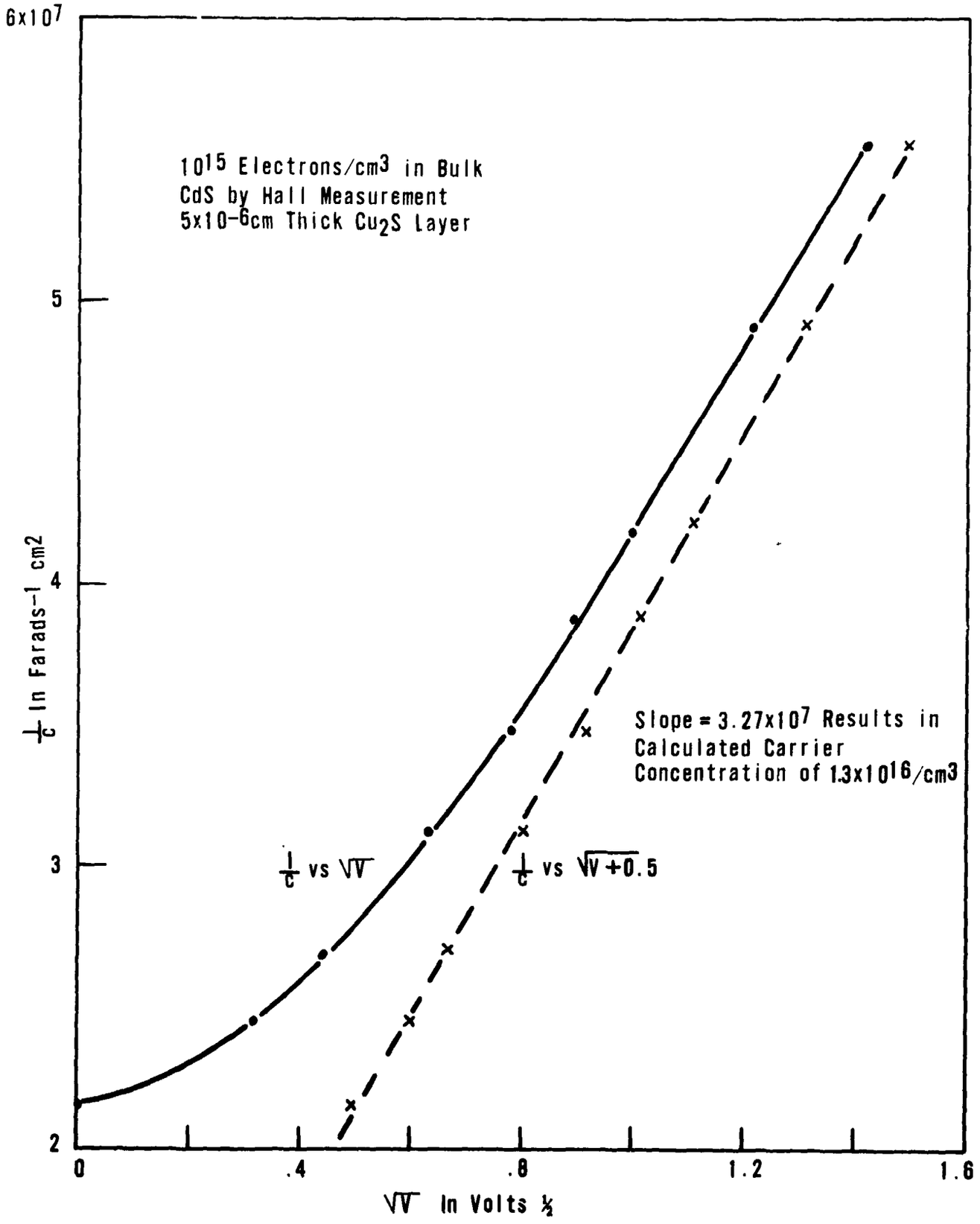

Figure 11 CdS SINGLE CRYSTAL CELL CAPACITANCE AS A FUNCTION OF REVERSE BIAS POTENTIAL

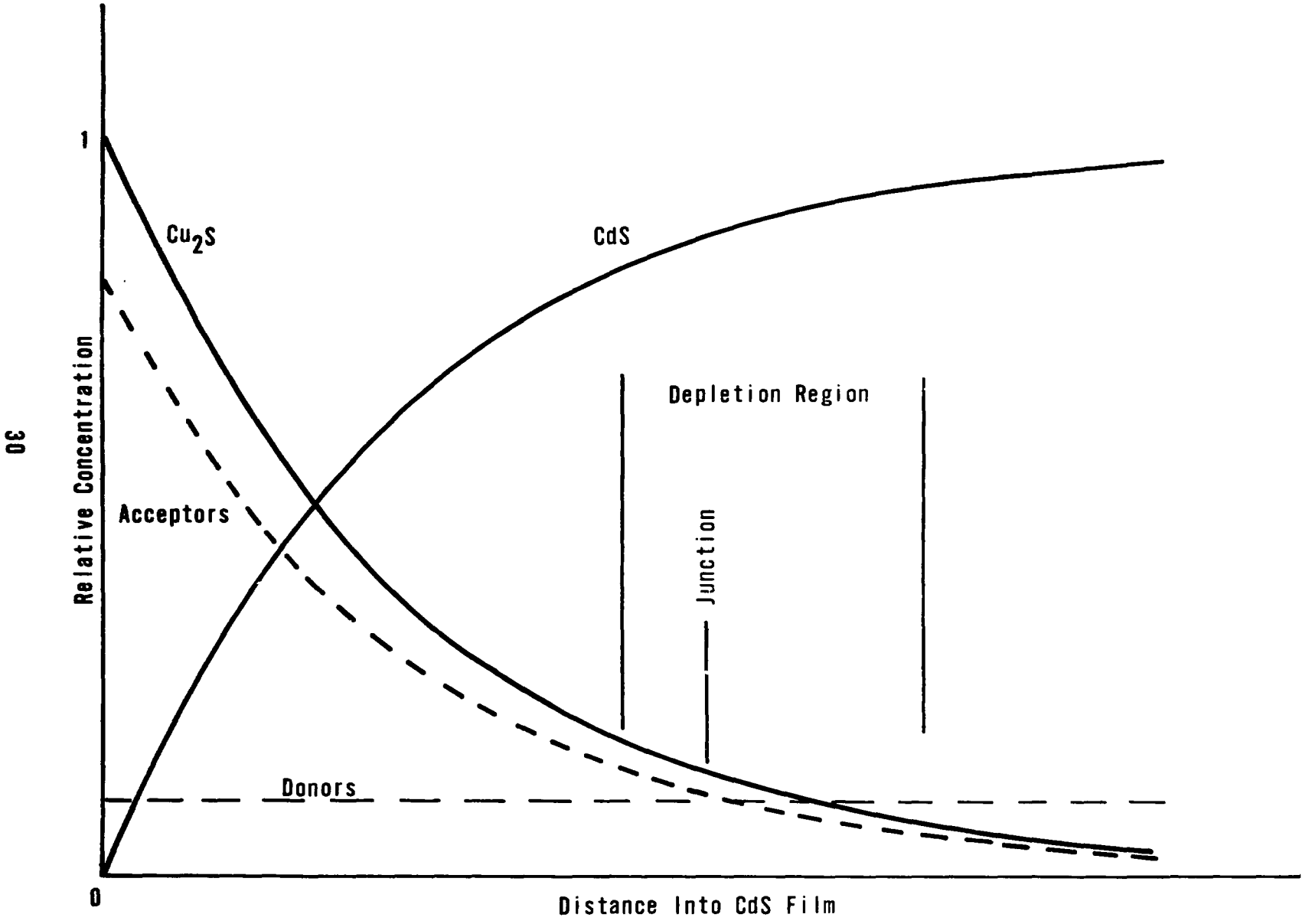

Figure 12 Schematic Representation Of CdS Cell

It was evident that the simple model does explain the structure of the response curves at low CdS electron concentrations.

Cells were also made from crystals with 10^{16} and 10^{17} carriers/cm^3 and the responses in Figures 9 and 10 show essentially the same behavior as that for the crystals with 10^{15} carriers/cm^3. The behavior between 2.2 and 2.3 eV is probably real, but is difficult to interpret without absorption coefficient data in CdS and Cu_2S in this range. The main conclusion to be drawn is that Cu_2S has a carrier concentration well above $10^{17}/cm^3$. We can also conclude that the gradient of Cu_2S is steep at the junction, and the junction behaves as a classical device in regard to capacitance.

Interface Materials

In order to provide an ohmic and tightly adhering contact between the CdS and the substrate, several interface materials were investigated. Sputtering techniques were used to provide metallic coatings on molybdenum. Greater adhesion of the coatings was anticipated. Electrodeposition of materials on molybdenum is difficult and generally lacks adhesion. The following results have been obtained:

Gold - Layers of gold less than 0.5 mils were sputtered on 2 mil molybdenum. Three such 3" x 3" substrates were put into a vacuum chamber. Glow discahrge was used to clean the surface before the CdS was evaporated. The CdS adhered well to the gold coated molybdenum. However, there was no indication of an improved ohmic contact since the control cell displayed a better I-V characteristic.

Silver - Layers of silver less than 0.5 mil were sputtered

on 2 mil molybdenum. Seven substrates were prepared and coated with CdS after a glow discharge cleaning. Two cells 4.8% and 4.6% resulted. In all cases, those with sputtered silver were better than the control. More cells were made using sputtered silver as an interface. The cells did not show a great superiority to those on plain molybdenum. However, there seems to be a tendency to higher currents on the silver coated substrates. The silver also provided a solderable tab to the molybdenum.

Zinc- Several attempts were made to sputter zinc on the molybdenum. The zinc would not deposit on the molybdenum.

Copper - Layers of copper less than 0.5 mil were sputtered onto 2 mil molybdenum. It adhered well. However, when the CdS was evaporated, it reacted with the copper to form a grainy brown film. This film was easily separated from the molybdenum, showing a gray layer next to the molybdenum.

1010 Sheet Steel - Some evaporations have been made on 2 mil 1010 sheet steel both silver coated and with roughened surface. Considerable curling and evidence of an appreciable series resistance in the final cells was noted.

Silver Coated Copper - Experiments with silver coated copper indicated that this combination would be usable. There is some curling but it is not excessive. Cells made on the copper-silver substrate have been comparable to those made on molybdenum. Careful control is necessary in many instances or the silver may separate from the copper. Due to the extra handling problems associated with the copper, molybdenum will continue to be used.

Nickel - The new nickel plating process reported under Solderable Contacts has been used to provide an interface material on the molybdenum. No immediate advantage was apparent.

Titanium - In the past titanium has been an attractive substrate material both because of its lower density and thermal expansion coefficient. However, cells made on titanium show a rapid deterioration after a period of about two weeks of apparent stability. Upon examination a darkening was found at the surface of the titanium when the CdS film was stripped.

Silver Coated Titanium - During this contract, cells were fabricated on sandblasted or sandblasted and silver (sputtered) coated titanium. All of these substrates were glow-discharged prior to CdS evaporation. The unexpected increase in stability in the titanium substrate cells prompted removal of some CdS for examinstion of the CdS-Ti interfaced. After one and two months, no discoloration was visible. So far, it has not been determined whether the surface treatment or the glow discharge is the important factor determining the improved condition.

Copper Base - Sputtered copper was also used as a base for layers of electroplated cadmium, zinc, silver, and additional copper. In each case, however, the copper tended to blister and peel from the molybdenum. For this reason, cells could not be made. It did suggest that copper foil or copper foil plated with various metals could be used as a substrate in place of the molybdenum.

Zinc on steel - Evaporations were attempted on galvanized metal. However, the CdS popped off the substrate before it could be removed from the vacuum chamber. The zinc coated metal could have provided an inexpensive, good ohmic contact to the CdS. The thermal expansion was too large to retain the CdS.

Doping

In the routine qualitative spectrographic analysis run on the CdS raw material silver was discovered. A quantitative analysis was run and in two of the three batches of CdS being used, silver was present in amounts as high as the ppm range. Whether it is there or not is still questionable. In a recent report on purified CdS, Eagle Picher [4] reported finding silver by emission spectrography but when a mass spectrograph was run in the same material, silver and several other elements were not found.

The cells made with silver doped CdS have not as yet displayed higher efficiencies than those without the added silver.

Effect of CdS Surface Preparations

The first few atomic layers of the CdS thin film surface provides the basis for formation of the p-type Copper Sulfide barrier layer. The nature of the surface, therefore, plays its role in the barrier layer formation and the resulting cell. To determine cell properties as a function of the CdS thin film surface, films were lapped with 600 and 1000 grit and Linde A polish. The structures of the surfaces were found

to be markedly different from each other and from that of the untreated CdS film. An indication of these differences is given by the pictures displayed below.

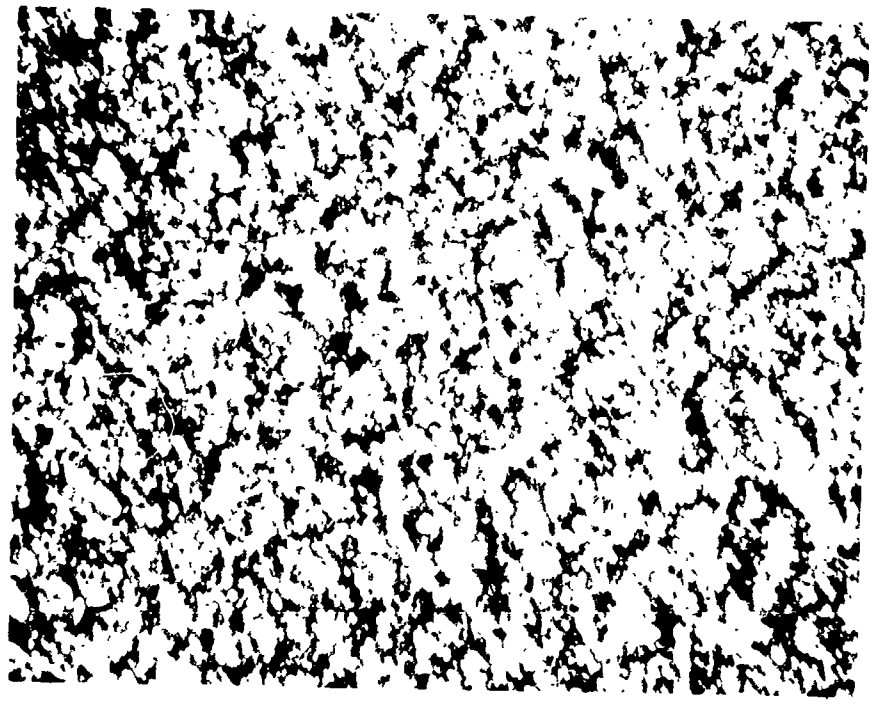

Figure 13

Untreated CdS Thin Film Surface. Magnification 320 X

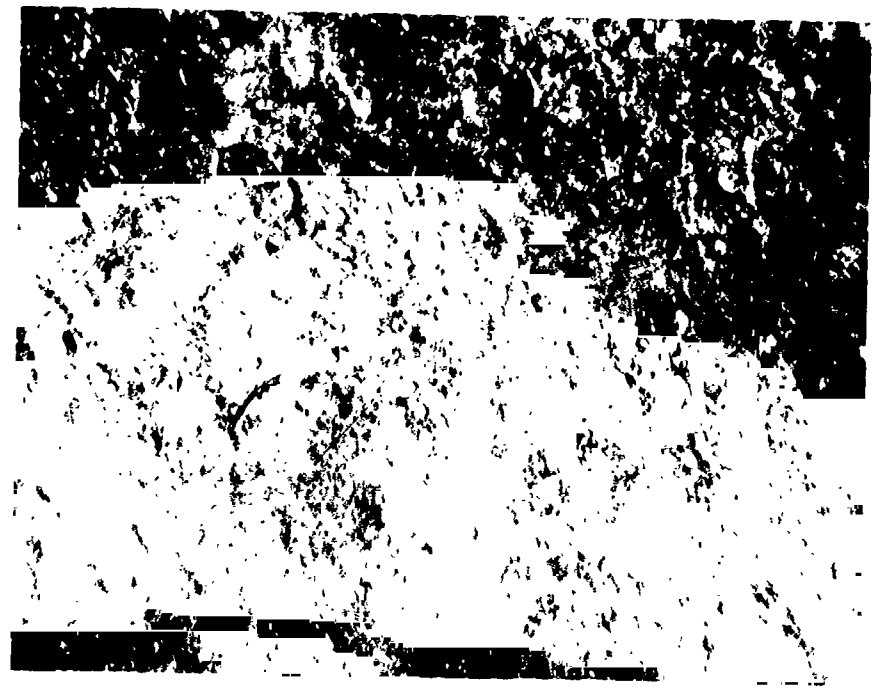

Figure 14

CdS Thin Film Surface Lapped with 600 Grit Magnification 320 X

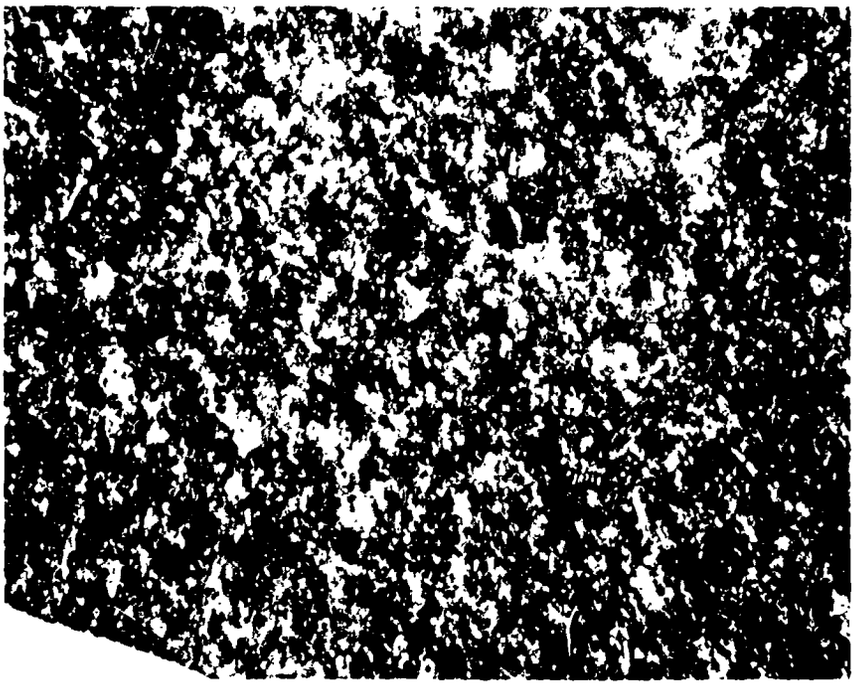

Figure 15

CdS Thin Film Surface Lapped with 1000 Grit

Magnification 320 X

Figure 16

CdS Thin Film Surface Polished with Linde A Polish

Magnification 320 X

Chemiplated barrier layers were formed on treated and untreated films. Measurements of the I-V characteristics indicate a dependence of open circuit voltage and short circuit current on the nature of the CdS film surface.

The parameter mostly affected is the short circuit current. The reason for this dependence is that the short circuit current directly depends on the thickness of the barrier layer and the number of n-type impurities in it. Both of these depend on the nature of the CdS into which the p-type layer is formed.

Etching rates for several etchants at various temperatures were determined. Unetched cells rarely equalled or exceeded the output of etched CdS cells.

An acid etch of the CdS surface can either reduce the current output to a value as low as 0.1 ma/cm^2 or enhance it by 20-40% over the current value achieved by making a cell with an untreated CdS surface.

Surfaces etched with a mixture of six parts glacial acetic acid, three parts fuming nitric acid and three parts distilled water gave very low current output if any at all. Excess sulfur was left behind on the surface of the CdS after the etching and the subsequent rinsing.

The results of etching the CdS surfaces with H_2SO_4 or HCl are comparable when the performance of the cells made is used as the criterion. The rate of etching is not linear with time. During the first 30 seconds there is considerable etching activity after which etching slows down. Table II shows the drop in weight loss after each of the six 30 second immersions. Etching rates were determined by calculating from the weight loss data.

Etching a CdS film for 60-80 seconds in concentrated H_2SO_4 or for 30 seconds in 1:1 HCl:H_2O is sufficient to provide a CdS surface which will give a cell of optimum performance. A shorter etch does not remove all the undesirable impurities from the CdS surface and a longer one causes deep etching along the grain boundaries of the crystallites. Such deep etching prepares the ground for a spread-out junction between the n-type

Table II

CdS Weight Loss During Etching

Immersion Number	Weight Loss For Each 20 Sec. Immersion			
	Sample Number			
	1	2	3	4
1	1.8mg	2.0mg	2.2mg	2.0mg
2	2.0mg	1.8mg	1.9mg	1.9mg
3	1.5mg	1.3mg	1.2mg	1.3mg
4	1.1mg	1.0mg	1.3mg	1.1mg
5	0.6mg	0.5mg	0.7mg	0.4mg
6	0.3mg	0.4mg	0.4mg	0.4mg

Etchant: Concentrated H_2SO_4

Etched Area = $4cm^2$

All samples were from same CdS film

Table III

Cell Data from Surface Treated Films

Sample		I_{sc}	V_{oc}	Area
1	(Not etched)	50 ma	.43V	4.0 cm^2
2	(Not etched)	52 ma	.43V	4.0 cm^2
25	(Etched in acetic acid, nitric acid, distilled H_2O 6:3:3)	0.2ma	.10V	4.0 cm^2
26	(Same as sample 25)	0.2ma	.30V	4.0cm^2
7	(Etched in conc. H_2SO_4 for 30 sec.)	59 ma	.43V	4.0 cm^2
8	(Etched in conc. H_2HO_4 for 30 sec.)	60 ma	.42V	4.0 cm^2
15	(Etched in conc. H_2SO_4 for 70 sec.)	80 ma	.43V	4.0 cm^2
16	(Etched in conc. H_2SO_4 for 70 sec.)	70 ma	.43V	4.0 cm^2
21	(Etched in 1:1 HCl:H_2O for 30 sec.)	68 ma	.44V	4.0 cm^2
22	(Etched in 1:1 HCl:H_2O for 30 sec.)	65 ma	.44V	4.0 cm^2
27	(Lapped with 600 Grit)	10 ma	.39V	4.0 cm^2
28	(Lapped with 600 Grit)	12 ma	.41V	4.0 cm^2
29	(Lapped with 1000 Grit)	15 ma	.39V	4.0 cm^2
30	(Lapped with 1000 Grit)	13 ma	.41V	4.0 cm^2
31	(Lapped with 600 & Etched)	18 ma	.41V	4.0 cm^2
32	(Lapped with 600 & Etched)	16 ma	.42V	4.0 cm^2
33	(Lapped with 1000 & Etched)	34 ma	.46V	4.0 cm^2
34	(Lapped with 1000 & Etched)	35 ma	.45V	4.0 cm^2
35	(Polished with Linde A)	38 ma	.46V	4.0 cm^2
36	(Polished & Etched)	42 ma	.44V	4.0 cm^2

CdS and p-type Copper Sulfide and ultimately causes shorting paths.

The current output of cells made from etched films is on the average 20 - 40% higher than the output of cells made of films with unetched surfaces. Cells were also made from films, the surfaces of which were lapped with 600 and 1000 grits and polished with Linde A polish, and finally from films which were lapped and polished as above and then etched for short intervals of time. Representative data can be seen in Table III.

All these preparations of the film prior to the barrier layer formation demonstrated that the nature of the surface does indeed play an important role in the output of the cell. However, from the performance point of view, the maximum output is achieved by etching the films in concentrated H_2SO_4 or solutions of HCl and distilled H_2O.

Semitransparent Cover Films

Semitransparent films were applied to the surface of the CdS solar cell for the purpose of providing increased collection efficiency. The layers to be investigated were CdTe, CuTe, Bi_2O_3 and Au.

Several evaporations of CdTe were made on glass to determine the best thickness and conductivity. The following table shows several of the CdTe films on glass. All of the films are n-type.

No.	Substrate Temp.	Filament Temp.	Doping	Thick-ness	Avg. Trans-Mission in Visible	Resistivity (ohm-cm)
23	300°C	950°C	.1% CuCl	800Å	56%	2.35×10^4
49	100°C	950°C	.1% CuCl 30% Te	400Å	28%	Not measured
50	100°C	950°C	.1% CuCl 30% Te	200Å	30%	Not measured
51	100°C	950°C	.1% CuCl 30% Te	100Å	92%	1.3×10^3

Films of CdTe were applied to eight CdS film cells according to the conditions reported for film No. 51 in the table. A large transmission variation of about 30% was apparent probably due to the difficulty in controlling the great excess of Te in the films. All of the coated cells suffered loss of both current and voltage. Their I-V curves displayed increased series resistance. Further work on the films as semitransparent collectors was abandoned.

Cell Testing Procedures

During the contract period it was discovered that a significant portion of the cells' efficiencies was not being realized as a result of the testing methods being employed. A radiation meter was used in conjunction with a RFL-2 tungsten lamp.

It also became evident that it is not correct to measure cells in 80 mw sunlight and then scale up the efficiencies by 20%. The missing light in 80 mw sunlight does not contribute significantly to cell operation.

A new test setup has been devised in order to gain better control in measuring cell performance and to produce a testing method consistant with that used by the contracting agency.

The test equipment incorporates a new test set-up with a light source patterned after that used at Lewis Research Laboratory, NASA. (Figure 17) The lamps are four 650 watt G.E. Sun Guns. Two types of lamps were considered. The General Electric bromine type and the Sylvania lamps which employ iodine. The two types of lamps (G.E. and Sylvania) were found to provide identical results. The G.E. lamps were selected because of their convenient size for the particular set-up, shorter filaments, and higher power. These shorter filaments are closer to being a point source.

The second important part of the test light set-up was the filter employed. It consists of an aluminum frame, and two 1/4" plate glass windows. The 12" x 12" windows are 2" apart. The space between the windows is completely filled with 0.1% copper sulfate solution. Actual useage of this filter was limited because of the attack of the solution on the aluminum. An all lucite box has been substituted. It has a reservior in the rear to supply solution to make up for evaporation. In addition a pyrex plate was mounted over the filter box to reduce the amount of infrared.

The standard cell used was calibrated by NASA. The CdS cell has been checked against other standards measured in sunlight. A silicon cell is also used for calibration purposes.

The I-V data is usually taken from the osciloscope display, but it can also be recorded on a x-y plotter.

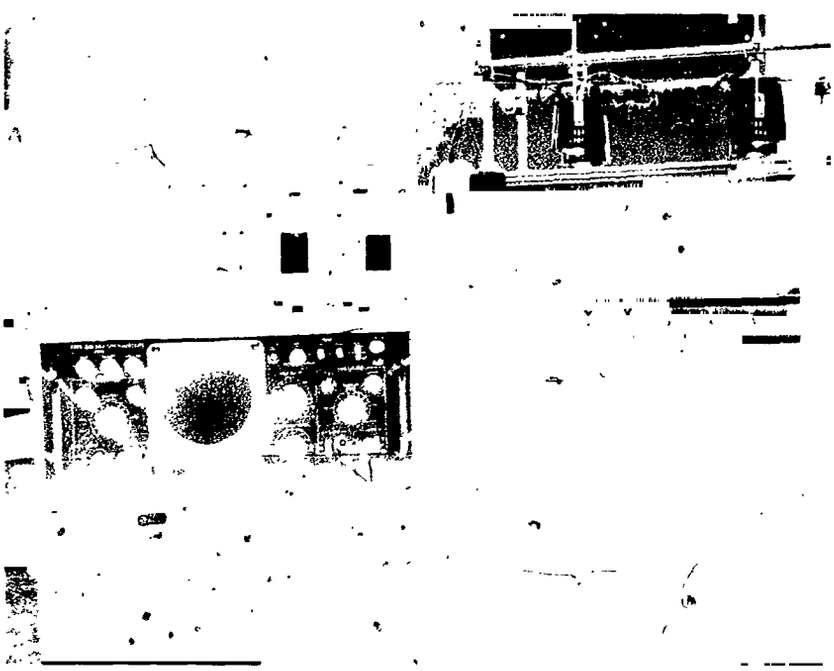

Figure 17

Simulation Solar Test Facility

This light source has been adopted as a simulated supply to facilitate the accumulation of meaningful test data from the various laboratories by means of a uniform testing procedure.

Pilot Line

During this contract over 500 3" x 3" cells were made on the pilot line. The highest efficient 3" x 3" cell with a laminated preformed grid was 5.4%. The most efficient 1" x 1" cell was 6.9%. The highest efficiency attained on a 3" x 3" cell with an electroplated grid was 4.7%.

Several difficulties were encountered during the operation of this pilot line. One was a double diode characteristic that appeared on the majority of cells evaporated over an extended period. It was traced to a thin layer that formed on the substrate when the substrate heater was turned on prior to evaporation. The formation of this film can be prevented by baking out the heater before the substrate is placed into the system. The nature of this has not been determined. This problem was more acute when the substrate to filament distance was shortened by approximately 30%.

The lower than expected efficiency is due to low cell voltage. Even though the current density has been steadily increasing, the efficiencies have not increased proportionally due to a loss in voltage. The most likely cause is the high carrier concentration that is being attained in the evaporated films. It approaches the 10^{18} carriers/cm^3 range.

The pilot line supplied films and cells for the various experiments run during the contract. Several cells were supplied to contract NAS3-6464 for various anti-reflective coating

experiments. It also supplied cells for delivery to NASA as specified in the contract. These cells were used for NASA in-house studies, calibrations, thermal-cycling tests, examples of the state-of-the-art; etc. Various sized cells in H-film, nylon, mylar-nylon, or open faced were delivered. The grids were affixed to the barrier by plastic, by thermo-compression, or electroplating.

Solderable Contacts to Molybdenum

A process has been developed by a subsidiary of The Harshaw Chemical Company that can be employed in cell fabrication. By use of this process, nickel coatings in the thousand angstrom range can be plated onto the molybdenum substrate. This eliminates the need for a two-mil thick nickel interface for welding leads to the molybdenum. Furthermore, this coating is extremely adherent and allows leads to be soldered or welded directly to the substrate. Wires soldered to the molybdenum broke before the solder joint. This method is expected to produce increased contact reliability. The nickel plate can be applied at any point in the cell process without damage to the cell.

Electrodeposited Grids

The major accomplishment in grid electroplating was the production of gridded cells with conversion efficiencies above 4%. The maximum efficiency of 4.7% was confirmed by NASA. This cell was stable for two months before being submitted to the NASA Project Manager for evaluation. Besides the contribution of advances in barrier formation, the efficiency increase

reflects improvements in electroplating techniques. The improvements are thicker photoresist masks, vigorous air agitation of the gold alloy plating bath, and low initial plating currents which are described below. In addition, these improvements have led to higher yields and more faborable physical appearance.

Photoresist Masking

Because of the difficulties in masking the pinholes and in grid line definition, a thicker photoresist coating was applied. This was accomplished by using a multiple coat method with decreasing spinner speed. Resulting masks have fewer pinholes requiring touch-up with a brush and photoresist. The effectiveness of this improvement can be judged by an almost complete elimination of "shorted" cells after grid electroplating. The thicker photoresist mask also gives a better defined grid because the lines remain of uniform width as the thickness of the line increases.

Electroplating Solutions

Modifications in the plating procedure have also contributed to the increased yield. The increase may be due to an improved contact between the cell and the gold grid. The procedure now requires an initial deposition of a thin 24K gold layer followed by a thicker high conductivity gold alloy layer. The initial plating current in both baths is 10% of the final plating current. This gradual increase in current allows the first layer of the plate to conform closely to the texture of the surface to be plated thus insuring a better contact. Air agitation of the

gold alloy bath has eliminated fogging.

A new high speed gold plating solution (Sel-Rex Temperex HD) was tested by plating a cell. Although this cell was merely a mechanical sample with low power output, no power decrease was observed. More important, photomicrographs showed that a deposit approximately twice as thick as normal was obtained in the same plating time. Normal deposits are 2.2 microns thick. However, when cells plated in a high speed gold plating solution were compared with cells plated in the standard manner, no difference was noted in electrical characteristics even though the high speed process produced a thicker plate. This is attributed to the greater conductivity of the gold alloy in the standard procedure.

It is possible to electroplate copper grids onto the cell barrier from the cuprous chloride barrier chemiplating solution. Since only the area to be gridded is exposed, the solution should not be injurious to the cell, and the initial copper layer was expected to prevent further barrier formation. A Hull cell[5,6,7] was used to determine the optimum plating conditions of 10ma/cm^2 at 25°C. Cells gridded by this method consistently produced low open circuit voltages. This is a direct confirmation of the results obtained with other copper plating solutions.

Yield

The yield based on 106 samples gridded in a six month period is 81% as shown on the bar graph in Figure 18. The "acceptance" line is drawn at -5% because this is a reasonable margin of error in cell testing. During one month 31 out of 33 cells were

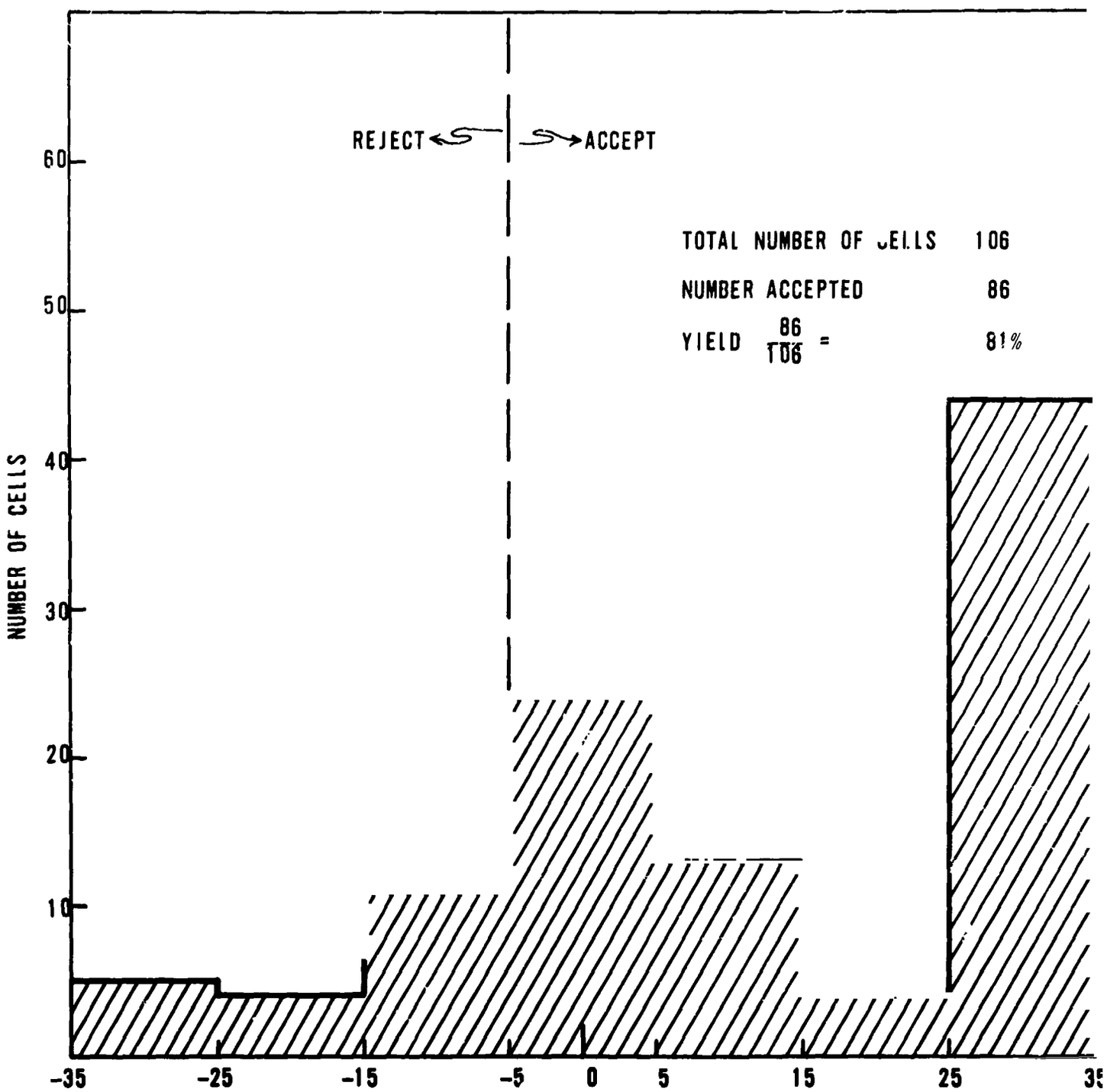

Figure 18 Electroplated Grid Yields

successfully gridded giving a yield of 94%. The yield results are based on efficiency before and after grid electroplating.

Electroformed Grids

The collector grid design and the method of attachment to the cell has been a continuing problem. Several approaches to an acceptable solution have been followed with respect to selection of the grid material such as gold, silver, copper, or nickel, and with respect to the method of attachment; i.e., lamination or electrodeposition.

Attachment of a metallic grid by the fusion of plastic during lamination provides the most efficient collection of current initially but degrades slowly during periods of temperature cycling. The electrodeposited grid provides a tenacious grid with very high reliability during thermal cycling.

Thermo-Compression Method

Although the efficiencies reported for the electrodeposited grid have reached the 5% level and that the total amount of materials per cell is less than any other workable method, it does involve several operational steps. A more rapid method of grid attachment that could attain the electrodeposited grid reliability would be an improvement. A Harshaw Company funded project has found that electroformed gold and other metals could be bonded to the cell surface by a thermo-compression method. Because of the success and simplicity of the procedure, it was felt that the compression bonding approach could advance the state-of-the-art and was worthy of further investigation of this contract.

The primary objective were (1) ease and rapidity of grid attachment, (2) stability and reliability; particularly with respect to thermal cycling, (3) lower gridding labor cost, (4) fabrication of cells with open face, and (5) numerous new methods of encapsulation.

The thermo-compression bonding procedure is essentially the positioning of the desired grid material on the face of the cell, placing the cell between two sheets of thin stock steel or other suitable stock, and then applying the heat and pressure in the range of 3000 p.s.i. simultaneously.

Bonding of gold grid to the CdS cell was quite successful with this method and samples were prepared for submission to NASA for temperature cycling tests. Other metal grids have been used and have been found to bond to a lessor degree. Further experimentation is expected to provide cells with the cheaper metal collectors such as copper and nickel.

One of the early cells (number 45-1) had a gold grid applied by thermal-compression and was sent to NASA for thermal cycling. The cycling consisted of 15 minutes light, and 30 minutes dark in a vacuum of 10^{-7} torr. The temperature cycle was approximately -60°C to +80°C.

This cell was open faced (no plastic). It was loaded for 1000 cycles, not loaded for 1000 cycles then loaded for 2000 cycles. The output of this cell has not changed after 4000 cycles.

Other cells sent for testing at NASA were distinguished by their copper grids. The grids are of the electroformed type. They were over 4% when tested at NASA.

These cells indicate that the thermo-compression bonding of the grid to the barrier without epoxy, adhesive, or plastic as bonding agents is quite satisfactory.

Experiments are being conducted using other metallic mesh materials.

In several instances the adhesion to the barrier surface was found to be excellent but the electrical properties of the cell indicated trouble. This was traced to the treatment given the grid before bonding. The simplest and least harmful procedure was gold plating on the under surface of the grid.

The transmission of the mesh when applied to the barrier surface was found to be reduced to 10% due to a spreading of the grid lines. This means that grids with less lires per inch should be used to compensate for the loss in active area.

Several 3" x 3" cells between 4 and 5% have been delivered to NASA for testing.

Density Measurement

As a quality control check of incoming material, the physical dimensions and weight of the Buckbee-Mears 70 line per inch gold grid were determined. From these figures, a density of 7.5 gms/cm^3 was obtained for the grid lines. This is less than one-half of the handbook value of 19.3 gms/cm^3. Also, the sheet resistivity of this grid was found to be ten times greater than the calculated value of 10^{-2} ohms per square. (Calculation based on resistivity of bulk gold.) Both the low density and the high resistivity illustrate the porous nature of the electroformed

grid. Attempts to prepare a sample of our electrodeposited grid for sheet resistivity measurement for comparison with the commercial grid have failed due to difficulties in removing the grid from the substrate. Some success has been obtained by etching away a thin copper substrate on which the grid has been electrodeposited. However, subsequent handling of the grid was very difficult.

Close-Spaced Vapor Transport

Introduction

Close-spaced vapor transport, a procedure whereby a thin semiconductive layer of material can be deposited onto a substrate, has been investigated.[8] There has been success in adapting this process to transport cadmium sulfide onto metal substrates. Thin films of polycrystalline cadmium sulfide suitable for processing into photovoltaic cells were produced.

Fixture Design

The first fixture consisted of lower and upper strip heater operating at different temperatures to provide the necessary temperature gradient. The films produced varied in thickness across the substrate indicating non-uniform heating. A shallow metal box was made to increase the powder area exposed to the substrate. The box was placed on a plate and in turn on the strip heater. This improved the heat distribution but was still not sufficiently uniform.

Because of the relatively small temperature gradient desired, the upper heater was replaced with a reflector. The reflector was mounted on a shaft to provide adjustment in the distance from the substrate. Sufficient control of the substrate temperature was obtained to cause the desired changes in the temperature gradient.

After a number of modifications to the lower heater failed to perform satisfactorily, it was decided that a combination heater and powder holder was needed. With this arrangement the powder was in direct contact with the heating element which developed a more constant and uniform heat. It also enabled the temperature to be monitored more accurately since the thermocouple was welded directly to the tantalum sheet heater. This was an improvement but because of film thickness requirements, the temperature had to be raised to increase the rate. The increase in temperature caused an area in the boat to be hotter. The resulting film displayed an identical "hot area" as a circle of slightly thicker film of different texture but poor adhesion. The flat heater sheet was made three inches wider, but the powder holder remained unchanged. This reduced the cooling of the edges of the powder holder. The change proved beneficial since a 3" x 3" film was made with reasonably uniform thickness at the operating temperature.

After a number of films were made, a crust formed at the section of the heater that was in contact with the powder. This crust seemed to have some effect on the transport rate. The

rate increased with the number of runs until the tantalum heater cracked. It was also believed that the CdS was becoming contaminated. A dark purple coloration appeared over the surface of the molybdenum substrate. This coating was thought to cause the double diode effect that appeared on the resultant cell curves. Therefore, an all quartz boat was incorporated into the system.

Much improvement was noted. A film of CdS on a 3" x 3" substrate produced a uniformity of ±4 microns across the surface of a film 27 microns thick. See Figure 19 for a sketch of the present fixture design.

Film Development

Initially, film thicknesses were in the range of 12 microns. Several cells made from these films resulted average efficiencies of 2.5%. However, a thicker film was desired to reduce the possibility of shorting during barrier formation. Therefore, since the temperature was the primary controlling factor, it was varied between 725 and 825°C, using various CdS powder. The transport rate for each powder increased or decreased with the temperature. For example, Sylvania CdS transported at approximately 20 mg per minute at 800°C and at 15 mg per minute at 760°C. General Electric CdS transported at approximately one-half that of Sylvania. After experimenting with several different powders, it was found that while Sylvania transported at the most desirable rate, the General Electric material seemed to give the best overall results. The operating temperature has

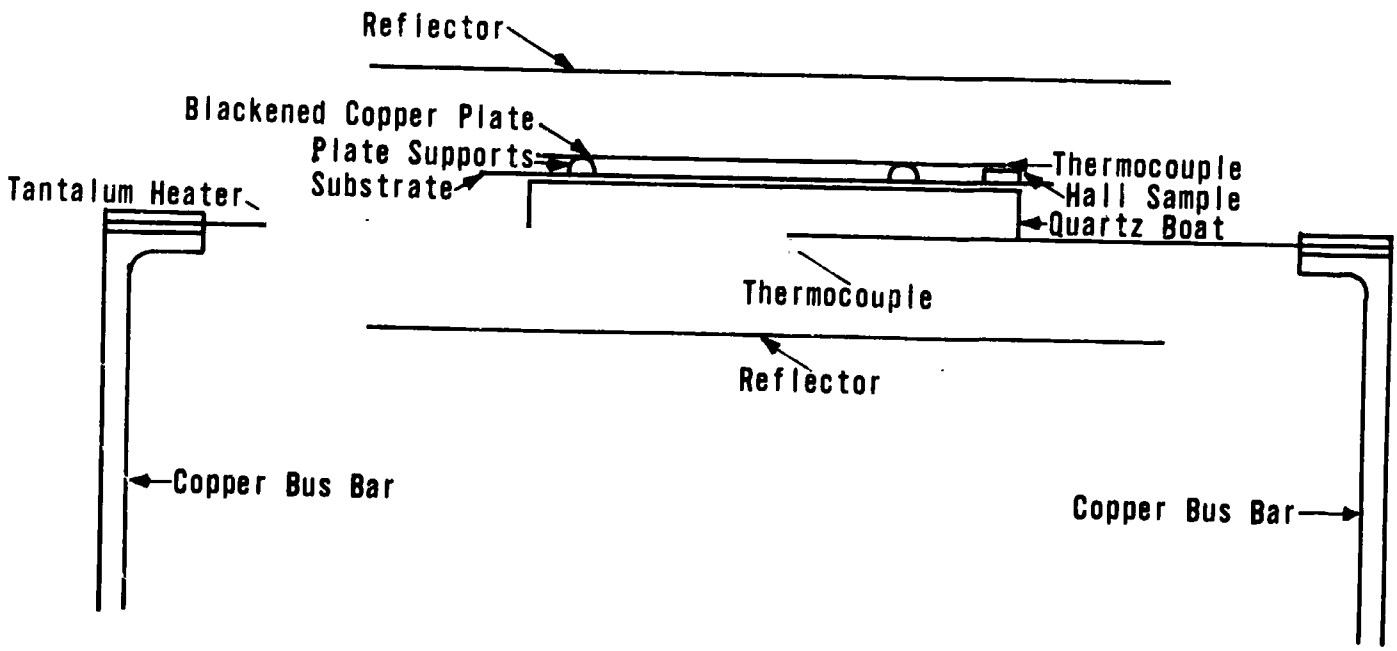

Figure 19 Vapor Transport Fixture

been approximately established at 775°C.

With films thickness around 24 microns, the adherance to the molybdenum substrate became a problem. Experiments were conducted to determine whether this procedure was more ameniable to metallic substrates other than molybdenum. The metals and alloys investigated are as follows:

1. Pure Copper — CdS attacked this substrate quite violently resulting in a flaky, black, non-adherent film. The substrate itself had holes in some areas.
2. 1010 Steel: — Resulting film was non-adherent. Material fell back into the boat. It was noted that the steel substrate lost weight during the run. It is also thought that the hexagonal crystallites in the film that formed were not CdS but FeS.
3. Invar: — The film had very poor adhesion and was quite brittle.
4. Copper Coated Molybdenum: — Resulting film was dark gray, very brittle with poor adherence to substrate.
5. Titanium: — Film was dark and somewhat glossy. Found to chip off as very small particles if the substrate was flexed.
6. Brass: — The entire film separated from the substrate as one sheet. The film

was approximately 4 mil thick with crystals 50 microns across.

Two runs were made with each metal. The titanium was selected as the only metal of this group that has shown promise.

Improvement in the adhesion to molybdenum was needed. Etched molybdenum was not satisfactory. Abrasion of the unetched molybdenum by sandblasting was investigated. Abrasion was the answer. Films up to 1 mil thicknesses can now be readily provided on sandblasted molybdenum substrates.

It was also found that the control of the film properties had improved. The Hall data taken from several runs under the same conditions verified this conclusion. The procedure is as follows: A sandblasted substrate is put in place over the CdS quartz container, then a piece of pyrex glass is positioned in juxtaposition. The CdS is deposited on the face of both materials simultaneously at 775°C at a one micron ambient pressure. The CdS on glass is used as the sample for the Hall measurements.

It has been found that by changing the dopant level the resistivity, mobility, carrier concentration can be controlled easily and reproducibly from run to run. Table I shows a sampling of Hall data for films doped with 0.05 wt. per cent indium sulfide. It was desired to control the film thicknesses between 15 and 20 microns. One film exceeded the range by one micron.

Table IV

Vapor Transport Film Characteristics

Resistivity (ohm-cm)	Mobility (cm^2-v-sec)	Carrier Conc. (cm-3)	Thickness (microns)
1.44	2.13	2.04×10^{18}	19
4.14	1.17	1.29×10^{18}	18
4.86	0.67	1.91×10^{18}	14
1.38	1.56	2.91×10^{18}	21
4.41	1.0	1.4×10^{18}	15
2.47	1.43	1.77×10^{18}	15
3.35	1.36	1.37×10^{18}	16

Good control of film properties is evident. Runs made later from a batch of similar composition gave:

Resistivity	Mobility	Carrier Conc.	Thickness
5.0	0.92	1.4×10^{18}	15
2.3	1.7	1.4×10^{18}	16
4.85	0.82	1.6×10^{18}	15.5

These data show that certain film properties can be predicted and produced. The following data were obtained on high resistivity films. Data on the mobilities or carrier concentrations were not obtainable.

Resistivity (ohm-cm)	Thickness (microns)
5.1×10^3	19
8.4×10^3	16
4.4×10^3	14

Resistivity (ohm-cm)	Thickness (microns)
2.9×10^3	13
4×10^3	16
2.6×10^3	19

Therefore, it can be seen that the vapor transport procedure can provide films with controlled properties within a factor of four.

Figures 20 and 21 compare an evaporated film with a transported film. Both films are c-axis oriented perpendicular to the substrate, but differ in that the transport film has 1) an obvious orientation in the plane of the photograph, 2) freedom from cracks, and 3) a low concentration of voids.

Cell Production

Initially all the cells were made from vapor transported cadmium films of 1 square inch areas. The barrier layer was formed by CuCl immersion method used for the evaporated films. The following data was taken from several of the cells.

Run #	CdS Film Thickness (microns)	CdS Film Resist (ohm-cm)	Cell V_{oc} Volts	j (ma/cm^2)	Cell Eff. (%)
22	11	1.2×10^3	.40	5.5	1.12
32	7	3.9×10^4	.40	6.9	1.90
33-C	12	1.9×10^3	.39	11.04	2.65*
33-2	12	1.9×10^3	.38	13.25	2.38*
35-1	12	0.95×10^2	.43	9.37	2.62*
35-2	12	0.95×10^2	.40	11.8	2.89*
35-3	12	0.95×10^2	.40	13.6	3.52*

*Efficiencies measured after lamination -

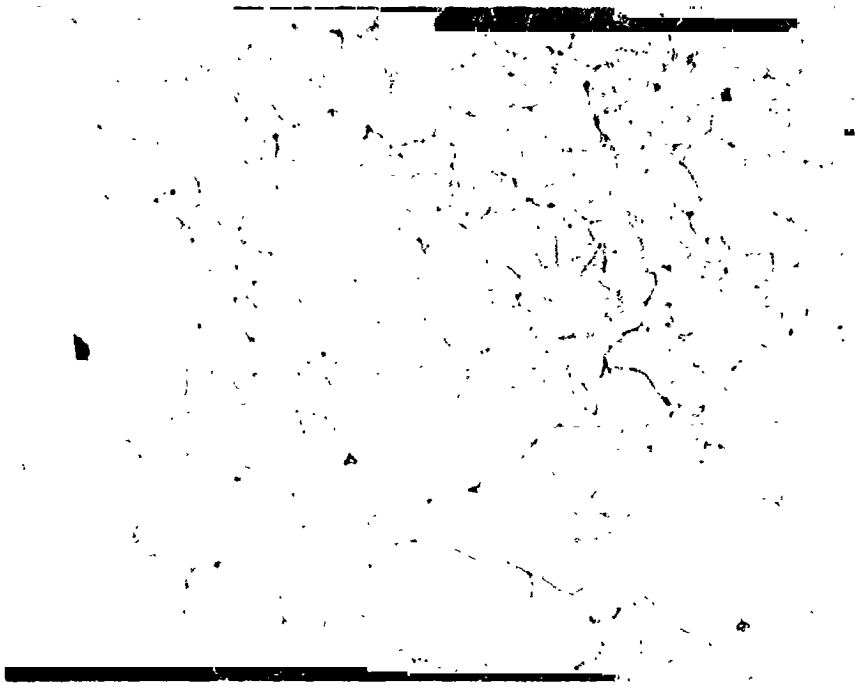

Figure 20

CdS Polycrystalline Evaporated Film

1000 x Magnification

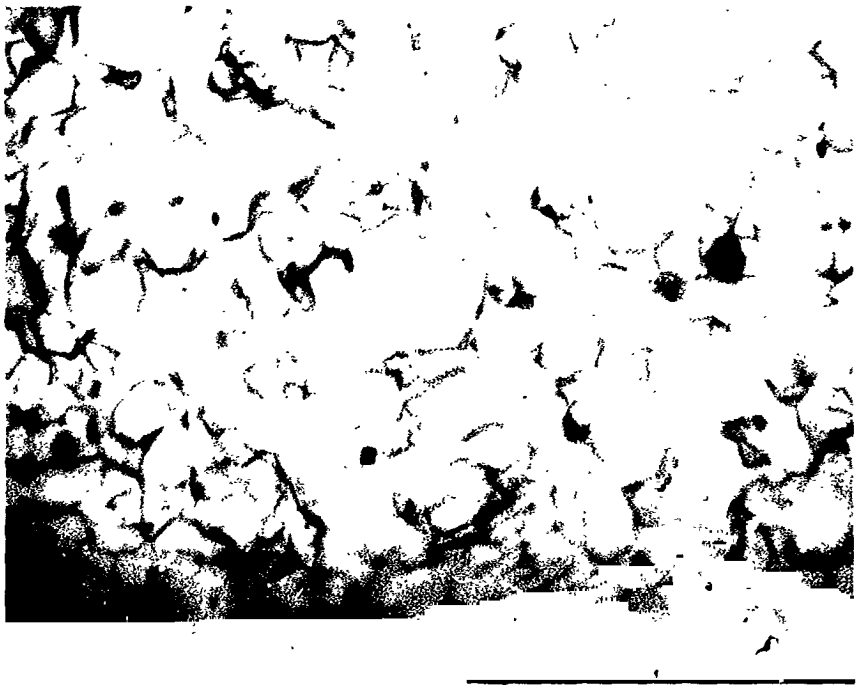

Figure 21

CdS Vapor Transported Film

1100 x Magnification

As additional cells were made and it was seen that the repeatibility was fairly good, several films were made with approximately twice the thickness. Cells were made and the following is typical data from the I-V curves.

		Initial Readings		Two Days Later	
No.	t (microns)	j (ma/cm^2)	Voc (volts)	j (ma/cm^2)	Voc (volts)
V-100-1	21	5.6	0.42	6.4	0.43
V-100-2	21	3.3	0.35	6.7	0.40
V-100-3	21	6.7	0.42	8.3	0.40
V-100-4	21	6.0	0.38	5.8	0.44
V-102-1	24	2.2	0.40	5.5	0.44
V-102-4	24	6.0	0.42	6.3	0.44
V-103-1	21	1.1	0.30	5.8	0.40
V-103-3	21	4.4	0.38	6.7	0.40
V-103-4	21	5.5	0.40	6.4	0.43
V-104-4	23	6.7	0.41	6.4	0.42
V-105-3	22	6.7	0.39	6.7	0.41

The above data shows that good control of ilm thickness can be maintained over a large range.

As is seen, the maximum cell efficiency from 1 square inch film was 3.5%. This was proof that a good cell could be made from the vapor transported film. Therefore experiements proceeded toward uniform 1 mil thick CdS film on a 3" x 3" substrate. This was done with the fixture shown in Figure 1. There were many films made on 3" x 3" substrates most of which are presently awaiting processing. A modified barrier procedure is needed for

film produced by this procedure. Of the small number that have been plated, the maximum efficiency attained was 3.6% with a short circuit current of 500 ma and open circuit voltage of 0.47 volts. Therefore, it is believed that this process can be further developed into an economic way of preparing films for processing into photovoltaic cells.

Spectral Response

The spectral response has been measured for a vapor transport type cell and compared with that of a typical cell from an evaporated film. Figure 22 is a plot of the data. As can be seen, there are differences especially in the lower light energy regions.

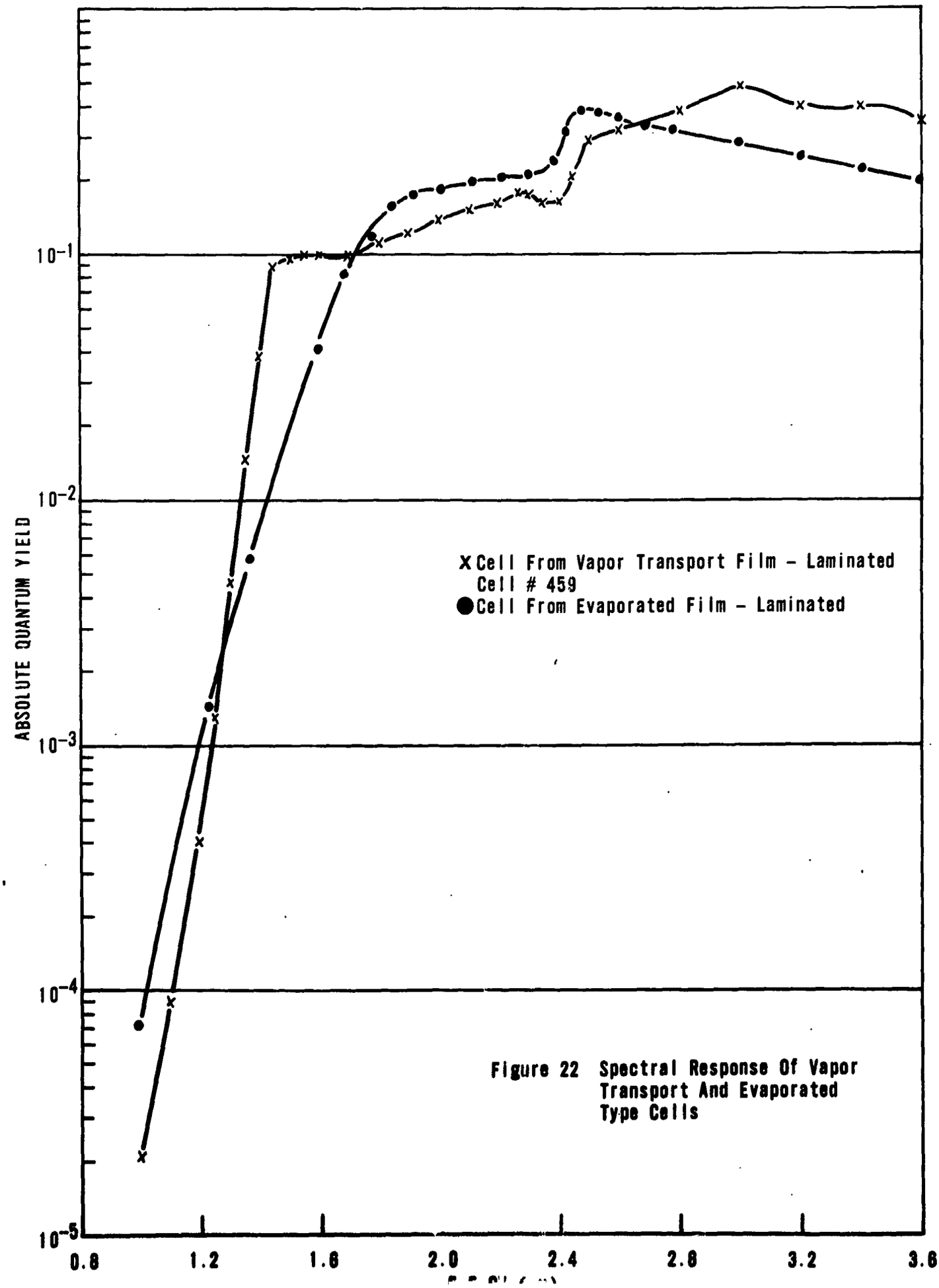

Figure 22 Spectral Response Of Vapor Transport And Evaporated Type Cells

References

(1) E. R. Hill and B. G. Keramidas, "A Model for the CdS Solar Cell," Photovoltaic Specialist Conference Goddard Space Flight Center, July 1965

(2) H. Kallman, B. Rosenberg, Phys. Rev. Vol. 97, pg. 1596 (1955)

(3) R. L. Clarke, Diffusion of Copper in Cadmium Sulfide Crystals, J. A. P. 30 (7) 957-960 July 1959

(4) Research in Purification and Single Crystal Growth of II-Vi Compounds. Eagle-Picher Co., Fourth Quarterly Progress Report, 15 Jan. 66 to 14 April 66 for ARL, WPAFB, Contract No. AF33(615)2947

(5) F. H. MacIntyre and R. O. Hull, Am. Electroplaters' Soc., Proceedings (1943)

(6) R. O. Hull, Am. Electroplaters' Soc. Proceedings (1939)

(7) Ibid., (1943)

(8) F. H. Nicoll, The Use of Close Spacing in Chemical-Transport Systems for Growing Epitaxial Layers of Semiconductros, R.C.A. Journal of Electrochemical Society, November 1963, Vol. 110, No. 11, pg. 465

Appendix - Calculations on Diffusion

The diffusion equation to be solved is,

$$D \frac{\partial^2 C}{\partial x^2} = \frac{\partial C}{\partial t} \qquad (1)$$

D = diffusion constant

x = distance from surface into the CdS film

The boundary conditions are

C = O at t = O

and

$C = C_1(1 - e^{-\lambda t})$ at x = O

C_o = bulk density of Cu_2S

$\lambda = \alpha C_o C_L$, the reaction constant at the CdS film surface

We call

$$C_o(1 - e^{-\lambda t}) = F(t) \qquad (2)$$

Then the general solution to (1) is, from Carslaw and Jager[1]

$$C(x,t) = \int_o^t F(\lambda) \frac{\partial}{\partial t} G(x, t - \lambda) d\lambda \qquad (3)$$

where $$G(x, t - \lambda) = \frac{2}{\pi} \int_{\frac{x}{2\sqrt{D(t-\lambda)}}}^{\infty} e^{-z^2} dz$$

Letting

$$u = \frac{x}{2\sqrt{D(t-\lambda)}}$$

and substituting for $\frac{\partial G}{\partial t}$, we find

$$C(x,t) = \frac{2}{\sqrt{\pi}} \int_{\frac{x}{2\sqrt{Dt}}}^{\infty} F\left(t - \frac{x^2}{4Du^2}\right) e^{-u^2} du$$

$$= \frac{2C_o}{\sqrt{\pi}} \int_{\frac{x}{2\sqrt{Dt}}}^{\infty} \left(1 - e^{\frac{\lambda x^2}{4Du^2} - \lambda t}\right) e^{-u^2} du$$

The solution to this is

$$C(x,t) = C_o \left\{ \operatorname{erfc} \frac{x}{2\sqrt{Dt}} - \frac{1}{2} e^{-\lambda t} \left[e^{ix\sqrt{\frac{D}{\lambda}}} \operatorname{erfc} \left(\frac{x}{2\sqrt{Dt}} - i\sqrt{\lambda t} \right) \right.\right.$$

$$\left.\left. + e^{-ix\sqrt{\frac{D}{\lambda}}} \operatorname{erfc} \left(\frac{x}{2\sqrt{Dt}} + i\sqrt{\lambda t} \right) \right] \right\}$$

The error function for complex argument is

$$\operatorname{erf}(a+ib) = \operatorname{erf} a + \frac{2}{\sqrt{\pi}} \int_0^b e^{y^2} (\sin 2ay + i\cos 2ay)\, dy$$

Thus, if a = 0

$$\operatorname{erf}(ib) = \frac{2i}{\sqrt{\pi}} \int_0^b e^{y^2} dy = \operatorname{erf}(-ib)$$

We are interested in two asymptotic cases, (a) for short times, and (b) for long times.

For short times, (a)

$$\sqrt{\lambda}t << \frac{x}{2\sqrt{Dt}}$$

And then,

$$C(x,t) \simeq C_o \left[\text{erfc} \quad \frac{x}{2\sqrt{Dt}}\right](1 - e^{-\lambda t} \cos x\sqrt{\frac{D}{\lambda}})$$

$e^{-\lambda t} \simeq 1$, giving

$$C(x,t) \simeq C_o \left[\text{erfc} \quad \frac{x}{2\sqrt{Dt}}\right](1 - \cos x\sqrt{\frac{D}{\lambda}})$$

Expanding the cosine term,

$$C(x,t) \simeq C_o \left[\text{erfc} \quad \frac{x}{2\sqrt{Dt}}\right]\left[\frac{x^2}{2} \quad \frac{(D)}{(\lambda)} - \frac{x^4}{24} \quad \frac{(D)^2}{(\lambda)^{2+}} \text{ ---}\right.$$

Keeping only the quadratic term

$$C(x,t) \simeq \frac{C_o D}{2\lambda} \quad x^2 \text{ erfc} \quad \frac{x}{2\sqrt{Dt}} = \frac{C_o D}{\lambda\pi} \quad x^2 \int_{\frac{x}{2\sqrt{Dt}}}^{\infty} e^{-z^2} dz$$

The total amount of diffusant is,

$$M(t) = \int_o^{\infty} C(x,t)dx \simeq \frac{C_o D}{\lambda\pi} \int_o^{\infty} x^2 dx \int_{\frac{x}{2\sqrt{Dt}}}^{\infty} e^{-z^2} dz$$

Letting $\frac{x}{2\sqrt{Dt}} = y$

$$M(t) \simeq \frac{8C_o D(Dt)^{3/2}}{\lambda \sqrt{\pi}} \int_o^\infty y^2 dy \int_y^\infty e^{-u^2} du$$

The integral is a number and consequently

$M(t) = At^{3/2}$ for short times. A = constant.

For long times $\sqrt{\lambda t} >> \frac{x}{2\sqrt{Dt}}$

Then

$$C(x,t) = C_o \text{ erfc } \frac{x}{2\sqrt{Dt}} = \frac{2C_o}{\sqrt{\pi}} \int_{\frac{x}{2\sqrt{Dt}}}^\infty e^{-z^2} dz$$

Again, the total amount of diffusant entering the surface is

$$M(t) = \int_o^\infty C(x,t)dx = \frac{2C_o}{\sqrt{\pi}} \int_o^\infty dx \int_{\frac{x}{2\sqrt{Dt}}}^\infty e^{-z^2} dz$$

Again, with $y = \frac{x}{2\sqrt{Dt}}$

$$\dot{M}(t) = \frac{4C_o\sqrt{Dt}}{\sqrt{\pi}} \int_o^\infty dy \int_y^\infty e^{-z^2} dz$$

$$= \frac{2C_o\sqrt{Dt}}{\sqrt{\pi}}$$

So, $M(t) = Bt^{1/2}$ for long times

where, B = constant